PHARMACIA

Pharmacia 72: 1–19
DOI 10.3897/pharmacia.72.e156784

Research Article

Development and characterization of furosemide-loaded binary amorphous solid dispersion to enhance solubility and dissolution for pediatric oral administration

Mays Fadhil Mohammed-Kadhum[1], Ghaidaa S. Hameed[1]

1 *Department of Pharmaceutics, College of Pharmacy, Mustansiriyah University, Baghdad, Iraq*

Corresponding author: Mays Fadhil Mohammed-Kadhum (fadhilmays@gmail.com)

Received 23 April 2025 ♦ **Accepted** 14 June 2025 ♦ **Published** 4 July 2025

Citation: Mohammed-Kadhum MF, Hameed GS (2025) Development and characterization of furosemide-loaded binary amorphous solid dispersion to enhance solubility and dissolution for pediatric oral administration. Pharmacia 72: 1–19. https://doi.org/10.3897/pharmacia.72.e156784

Abstract

Binary co-amorphous systems, as solid dispersions of an active pharmaceutical ingredient with low molecular weight excipients, improve solubility, physical stability, and bioavailability relative to crystalline forms. This study aimed to enhance the solubility and dissolution of furosemide by developing a binary amorphous solid dispersion (BASD) and formulating it into granules for pediatric administration via a straw. Furosemide was blended with hydroxy methylcellulose E6, polyvinylpyrrolidone K30 (PVP), or Soluplus® in a 1:2 ratio using solvent evaporation, and the best formulation was produced via wet granulation. The furosemide-loaded BASD-PVP K30 (Formula F) demonstrated superior FTIR, DSC, and XRPD profiles. In vitro release testing showed that over 87.18% of furosemide was liberated within 120 minutes in a water solution containing 0.1% Tween 80. Moreover, the granules of Formula F9 exhibited excellent flow, disintegrated within 5–6 seconds, and released 79.86% of furosemide within four hours in a two-step dissolution study (0.1 N HCl and pH 6.8 phosphate buffer). Stability testing over three months revealed no perceptible changes in appearance or drug content. These findings support the effectiveness of BASD granules in enhancing furosemide dissolution and their potential for pediatric administration.

Keywords

furosemide, hydroxy methylcellulose, polyvinylpyrrolidone, Soluplus, binary amorphous solid dispersion

Introduction

Pediatric heart failure constitutes a significant source of morbidity and mortality in children (Masarone et al. 2017). Congestion and fluid retention are characteristic features of decompensated heart failure and the primary cause of the hospitalization of individuals with this condition. Diuretics have been utilized in heart failure for decades and continue to be the cornerstone of modern heart failure care. Loop diuretics are the preferred diuretic and have received a class I recommendation from clinical guidelines for alleviating congestion symptoms (Wu et al. 2024).

Furosemide, as a loop diuretic, is a first-line therapy for acute heart failure, including pediatric patients

(Abraham et al. 2021; Biegus et al. 2023). It primarily works by inhibiting the $Na^+/K^+/2Cl^-$ cotransporter in the thick ascending limb of the Loop of Henle in the kidneys, which leads to a reduction in the symptoms of excessive fluid accumulation, enhances the resolution of pulmonary congestion, and relieves dyspnea (Eid et al. 2021; McMahon and Chawla 2021). The main indication in pediatrics is to reduce excessive fluid retention and restore proper sodium chloride and water balance for those with chronic heart failure (Lava et al. 2023). Various loop diuretics have distinct pharmacological characteristics and pharmacokinetic profiles. When administered orally, loop diuretics are absorbed from the gastrointestinal tract, exhibiting varying degrees of bioavailability depending on the specific drug. Furosemide has variable absorption and, on average, a reduced bioavailability of 50% (Sica 2003). During acute decompensated heart failure, significant venous congestion and intestinal edema can further impede the absorption of loop diuretics (Ikeda et al. 2021). Thus, enhancing the oral bioavailability of furosemide is a crucial consideration when designing a new oral dosage form for this medication.

Drug solubilization is a crucial process for the systemic absorption of orally given medicines (Jaafar et al. 2020). Regrettably, a significant proportion of commercial pharmaceuticals (~40%) and those in the research and development pipeline (~90%) exhibit poor water solubility, including furosemide (Ku 2008; Babu and Nangia 2011; Benet et al. 2011). Furosemide is a carboxylic acid derivative with a weak acidity, as indicated by its pKa value of 3.48. Its solubility in water increases as the pH level rises, going from 0.18 mg/mL at pH 2.3 to 13.36 mg/mL at pH 10.0 (Koh et al. 2021; Lomba et al. 2023). It has a 1.5–2 hour elimination half-life (Pandey et al. 2022). Furosemide is classified as a class IV drug according to the Biopharmaceutical Classification System due to its low solubility in water and limited ability to pass through cell membranes (poor permeability) (Van der Merwe 2021). Various approaches improve the solubility of furosemide. These approaches include particle size reduction, nanosuspension, surfactants, salt formation, pH modification, solid dispersion, co-crystals, amorphous compound formation, and inclusion complexes (Aldahhan and Radhi 2020; Ainurofiq et al. 2021).

The solubility and dissolution rate of weakly water-soluble pharmaceuticals can be effectively enhanced by manufacturing them as amorphous solid dispersions (ASDs) (Van Den Mooter 2012; Brough and Williams III 2013). ASD is a solid dispersion wherein the active ingredient is included inside an excipient matrix in a predominantly amorphous state. The amorphous form of the medication in ASDs is essential for enhancing its solubility (Newman et al. 2017). In its amorphous state, the medication needs no energy to disrupt the crystalline structure. Consequently, in comparison to the crystalline form, the amorphous form of numerous poorly water-soluble medicines can attain significantly greater apparent solubility and considerably enhanced dissolving rates (Vaka et al. 2014). ASDs are known to enhance membrane flux due to elevated supersaturation, hence improving bioavailability (Miller et al. 2012; Newman et al. 2012). ASDs exhibit increased wettability owing to the incorporation of hydrophilic polymers (Vasconcelos et al. 2007).

Solid dispersions are categorized as first, second, or third generation based on their formulation composition (Tekade and Yadav 2020). Solid dispersions utilizing crystalline carriers represent the first generation (Kim et al. 2011). Their drug release rate is typically slower than the two generations of solid dispersions. ASDs are comprised of amorphous medication and polymer and represent the second generation (Bindhani and Mohapatra 2018). ASD formulations may additionally use supplementary excipients, including extra polymers and/or surfactants, to further improve drug release and stability. These ASDs are classified as third generation (Vo et al. 2013). ASD formulations have attracted considerable interest in academia and industry over the past decade due to their solubility and dissolution benefits (Vasconcelos et al. 2016; Jermain et al. 2018).

Hydroxypropylmethylcellulose (HPMC)-E6, polyvinylpyrrolidone (PVP)-K30, and Soluplus® (a graft copolymer consisting of polyvinyl caprolactam, polyvinyl acetate, and polyethylene glycol) are carriers used in ASDs (Iyer et al. 2021). This approach distributes the active pharmaceutical ingredient (API) within a carrier compound, often a water-soluble polymer excipient, to create a multi-component matrix. When the API is dispersed within the carrier matrix, it is in a higher energy state than its more stable crystalline form. The solubility and dissolution rate of the mixed ASD phase are increased because the API has a larger surface area exposed to the solvent (Saboo et al. 2021; Walden et al. 2021). The PVP-K30 was utilized as a carrier to create an innovative ASD of furosemide (Zhang et al. 2022). The PVP-K30 is one of the most commonly utilized hydrophilic polymers in the formulation of ASD because of its capacity to prevent drug crystallization, enhancing the dissolution rate (dos Santos et al. 2021).

In Iraq and most countries, the registered oral dosage form of furosemide is a 40 mg oral tablet. To obtain the requisite pediatric dosage, it is essential to pulverize commercially available tablets, combine the powder with a filler, and make capsules extemporaneously in a pharmacy. Subsequently, the capsule must be opened before use and combined with baby food or drink before administration (Fadda et al. 2024).

Liquid formulations are favored due to their flexible dosing, enhanced adherence by patients and caregivers, and greater pharmacy compounding ease (Nunn and Williams 2005; Cram et al. 2009). Oral liquid formulations containing furosemide are often not recommended for pediatric use due to the vehicle's elevated ethanol concentration. For instance, Frusol 20 mg/5 mL oral solution (Rosemont Pharmaceuticals Ltd.; UK)

comprises 10% ethanol, Impugan 10 mg/mL oral drops (Actavis Group hf.; Sweden) contain 9.8% ethanol, and Lasix® liquid 10 mg/mL (Sanofi-Aventis, Germany) has 11.9% ethanol. The utilization of ethanol as an excipient in pediatric medications fails to meet the standard criteria for pediatric formulations (Sweetman and Martindale 2009) and is deemed inappropriate by pediatric drug committees, regulatory bodies, and published literature (Salunke et al. 2012; Salunke et al. 2013; Zahálka et al. 2018) (Mahmood et al. 2022).

To overcome these limitations, this study focuses on developing a suitable and non-toxic oral dosage form for pediatric formulations, which stems from the lack of suitable oral dosage forms for furosemide in this population. This study introduces a novel formulation, namely, binary co-amorphous solid dispersion (BASD) of furosemide, which will later be dispersed as granules and filled into straws. Using BASD enhances the solubility, stability, and disintegration time of furosemide. Using straws enhances patient compliance, ensures uniform dosage, improves the appearance and flavor of the final product, and increases patient compliance.

Materials and methods

Materials

Furosemide was purchased from Changzhou Yabang Pharmaceutical Co., Ltd. (China) with a purity of > 99%. PVP-K30 was obtained from HiMedia Laboratories (India). Soluplus® was sourced from BASF Pharmaceutical Industries (Germany). HPMC-E6 was purchased from Macklin Co., Ltd. (China). Tween 80 was procured from HiMedia Laboratories (Chemicals) Pvt. Ltd. (India), and methanol was obtained from Sisco Research Laboratories Pvt. Ltd. (India). Talc and magnesium stearate were acquired from Alladin Industrial Co. (Shanghai, China), while mannitol was supplied by Alpha Chemika (India). Hydrochloric acid (HCl) was purchased from Thomas Baker (Chemicals) Pvt. Ltd. (India). Aerosil and crospovidone were sourced from Shanghai-Ruizheng and Aladdin Chemistry Co., Ltd. (China), respectively. Pullulan polysaccharide was obtained from Aladdin (Shanghai, China). Sodium bicarbonate was purchased from Samara Drug Industry (Iraq), and calcium carbonate was supplied by HiMedia Laboratories (India). Strawberry coloring and flavoring agents were obtained from Fluka Chemika (Switzerland). All other chemicals and solvents used in this study were of analytical grade.

Pre-formulation of furosemide

Preparation of physical mixtures

As shown in Table 1, furosemide was mixed in a 1:2 ratio with either HPMC-E6, PVP-K30, or Soluplus®. The components were accurately weighed and thoroughly mixed in a glass mortar for 10 minutes at room temperature (25 °C) until a uniform blend was obtained. The prepared mixtures were stored in desiccators for further analysis (Alwossabi et al. 2022).

Table 1. Physical mixture formulas.

Formulation	A	B	C
Furosemide	12 mg	12 mg	12 mg
HPMC-E6	24 mg		
PVP-K30		24 mg	
Soluplus®			24 mg

HPMC: hydroxypropyl methylcellulose; PVP: polyvinylpyrrolidone.

Preparation of solid dispersion formulas

As shown in Table 2, furosemide as a pure active pharmaceutical ingredient (API) was mixed with HPMC-E6, PVP-K30, or Soluplus®, then dissolved in 20 mL of methanol at a 1:2 (drug:polymer) weight ratio.

Table 2. Binary solid dispersion formulas.

Formulation	D	E	F	G	H
Methanol	20 mL	20 mL	20 mL	20 mL	
HPMC-E6		24 mg			
PVP-K30			24 mg		
soluplus®				24 mg	
Furosemide	12 mg	12 mg	12 mg	12 mg	12 mg

SE: solvent evaporation; HPMC: hydroxypropyl methylcellulose; PVP: polyvinylpyrrolidone.

The solvent was evaporated using a rotating vacuum evaporator (Buchi Interface I-300 Pro, Germany) at 50 °C and 150 mbar for 30 minutes to produce a binary amorphous solid dispersion (BASD).

The dried material was crushed, sieved to achieve a uniform particle size, and further dried in an oven at 40 °C for 24 hours. The resulting ASDs were stored in desiccators for characterization (Naama et al. 2025).

Percentage yield of the prepared BASD of furosemide

The percentage yield for each type of BASD was calculated by comparing the actual weight of the acquired ASD to its theoretical weight using the following equation (Al-Hassani and Al-Khedairy 2021):

$$\text{Percentage yield} = \frac{\text{Practical mass of the BASD}}{\text{Theoretical mass of the polymer and drug utilized in the formulation}} \times 100$$

Drug content of the prepared solid dispersion

Approximately 36 mg of each formula (Tables 1, 2) was added to 100 mL of deionized water containing 0.1% Tween 80. The mixture was stirred for 30 minutes at 100 RPM. The resulting solution was filtered using a 0.45 µm filter syringe (filtraTECH, France), diluted with

deionized water and 0.1% Tween 80, and analyzed by spectrophotometry (Shimadzu UV-1650PC, Japan) at a λ_{max} of 277 nm (Hatem and Ali 2023; Nser et al. 2023).

Differential scanning calorimetry (DSC)

Furosemide melting points were assessed by DSC (Shimadzu 60, Japan) for all formulas (Tables 1, 2) (Ruponen et al. 2021). The procedure was as follows: 5 mg of each formula was placed in an aluminum pan and scanned at increments of 10 °C/min from 10 to 300 °C under a nitrogen purge. The thermograms were analyzed using Shimadzu TA-60 software (Sabry et al. 2021).

Powder X-ray diffractometry (PXRD)

All formulas (Tables 1, 2) were assessed using PXRD (XRD6000, Shimadzu, Japan). Patterns were collected over a 2θ range of 5° to 90°, with an operational voltage of 40 kV and a current of 30 mA for X-ray diffraction (Kadhim and Rajab 2022).

Fourier transform infrared spectroscopy (FTIR)

All formulas (Tables 1, 2) were analyzed using FTIR (Shimadzu 8300, Japan). The FTIR spectra were recorded using the KBr disc method and scanned in the range of 4,000 to 400 nm (Hatem and Ali 2023; Kaoud et al. 2024; Lateef et al. 2024).

Determination of saturated solubility

The phase solubility method was used to determine the saturated solubility. An excess amount (50 mg) of furosemide from each formula (Tables 1, 2) was agitated in 10 mL of deionized water containing 0.1% Tween 80 at 25 °C for 72 hours at 200 RPM in screw-capped tubes. The samples were centrifuged (Hettich, Germany) at 5,000 RPM for 30 minutes. The resulting solutions were filtered using 0.45 µm sterile syringe-driven filters and analyzed at λ_{max} 277 nm using a UV spectrophotometer (Gulsun et al. 2018; Dalal et al. 2021; Pantwalawalkar et al. 2021; Akram et al. 2022; Maded et al. 2024b).

In vitro dissolution studies

Dissolution studies were conducted using a USP Apparatus II (paddle method) at 37 °C (±0.5 °C). Samples from each formula (Tables 1, 2) were agitated at 50 RPM in 250 mL of a dissolution medium composed of deionized water and 0.1% Tween 80. All experiments were conducted in triplicate. At time intervals of 15, 30, 45, 60, and 120 minutes, 5 mL samples were withdrawn through a 0.45 µm filter syringe and replaced with an equal volume of pre-warmed (37 °C) fresh medium. The samples were analyzed at λ_{max} 277 nm using a UV spectrophotometer (Butreddy et al. 2021; Nupur et al. 2023; Maded et al. 2024a).

Selection of the best BASD formula

The most effective binary amorphous solid dispersion (BASD) formulation was selected based on the results of differential scanning calorimetry (DSC), powder X-ray diffraction (PXRD), Fourier transform infrared spectroscopy (FTIR), saturated solubility testing, and in vitro dissolution studies. The formulation demonstrating superior performance across these parameters was chosen for further processing into granules.

Field emission-scanning electron microscopy (FESEM)

Using gold-coated samples, the FESEM (CARL ZEISS EVO MA10, Cambridge, UK) analyzed the particle size and surface morphology of all formulas (Tables 1, 2) (Vaid and Jindal 2022; Aziz and Sabar 2025).

Formulation of furosemide BASD as granules

Preparation

The wet granulation method was used to prepare furosemide-PVP BASD granules. The furosemide solid dispersion, equivalent to 12 mg of furosemide, was weighed and mixed with super-disintegrants (crospovidone) and Aerosil® 1.0%. Calcium carbonate 1.0% was used as a release booster, and strawberry flavor was added to improve taste and color. The final blend was diluted with mannitol. The quantities of each component are shown in Table 3.

The dough mass was prepared by adding 1 mL of distilled water. The bulk was sieved using a 2 mm sieve (Areej Al-Furat AFC lab test sieve, Iraq), then dried in an oven at 40 °C for 30 minutes. Afterward, 6 grams of granules equivalent to 12 mg of furosemide were hand-loaded into semi-closed, commercially available plastic straws (Kix straw, Iran) for

Table 3. Composition of the prepared granules.

Ingredients (mg)	F1	F2	F3	F4	F5	F6	F7	F8	F9	F10
BASD	36	36	36	36	36	36	36	36	36	36
Mannitol	5454	5454	5454	5604	5454	5604	5394	5544	5394	5544
Crospovidone			300 (5%)	150 (2.5%)	300 (5%)	150 (2.5%)	300 (5%)	150 (2.5%)	300 (5%)	150 (2.5%)
Pullulan polysaccarides	300 (5%)	300 (5%)								
Talk 1%	60	60	60	60	60	60	60	60	60	60
Magnesium stearate 1%	60	60	60	60	60	60	60	60	60	60
Sodium bicarb 1%		60			60	60			60	60
Calcium carbonate 1%	60		60	60			60	60		
Flavouring & coloring agent 0.5%	30	30	30	30	30	30	30	30	30	30
Aerosil 1%							60	60	60	60
Total	6g	6g	6g	6g	6g	6g	6g	6g	6g	6g

oral delivery (190 mm long, 8 mm wide) for children. The product was stored in aluminum foil with a desiccant in an airtight container for evaluation (Divya et al. 2020). Fig. 1 illustrates the preparation method.

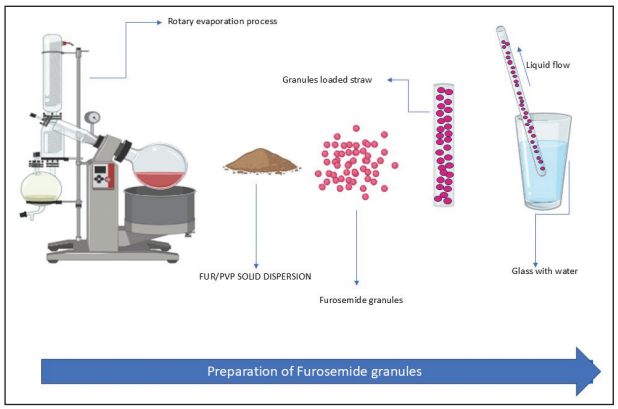

Figure 1. Preparation steps of furosemide-BASD granules.

Evaluation of the granules

The angle of repose

The prepared granules flow through the funnel until the top of the conical pile reaches the tip; the conical pile's radius and height are measured. The angle of repose is calculated using the following equation (Müller et al. 2021):

$$Tang_{\theta} = h/r$$

The variables are the angle of repose (θ), pile height (h), and pile radius (r).

Bulk density

Ten grams of granules were inserted into a dry 25 ml graduated cylinder. The granules were gently leveled without compression and measured for their unsettled volume (V_0), given in g/ml; bulk density was calculated using the following equation (Pharmacopeia 2018):

$$P_{bulk} = \frac{M}{V_o}$$

Where apparent bulk density (P_{bulk}), sample weight (M), and apparent powder volume (Vo).

Tapped density

Ten grams of granules in a 25 ml graduated cylinder were manually tapped 100 times until they reached a constant capacity, estimated as the tapped volume. The tapped density was calculated from the powder blend mass and tapped volume, as seen in the equation (Pharmacopeia 2018).

$$P_{tab} = \frac{M}{V_t}$$

Where P_{tab} indicates tapped density, M indicates sample weight, and V_t indicates tapped powder volume.

Carr's index: compressibility index

The flowability can be assessed by comparing the bulk density before tapping (P_{bulk}) and tapped density (P_{tab}). The proportion of Carr's index was determined based on the following equation (Alwan and Ibrahim 2021):

$$\text{Carr's index} = \frac{P_{tab} - P_{bulk}}{P_{tab}} \times 100$$

Haunser's ratio

Hausner's ratio is an essential parameter for assessing the flow characteristics of powders and granules; this can be computed using the following formula (Mudrić et al. 2021):

$$\text{Haunser's ratio} = \frac{P_{bulk}}{P_{tab}}$$

In vitro dissolution study

The dissolution study was performed under two conditions: in water and in a two-step dissolution medium. In water, an unconventional test measured drug release during sipping. A straw containing prepared granules was immersed in 9 mL of purified water. After disintegration, samples were filtered using 0.45 µm syringe filters and examined using a UV spectrophotometer at λ_{max} of 276.5 nm (Simšič et al. 2021).

A paddle-equipped dissolution apparatus II was used to measure granule dissolution in 0.1 N HCl (pH 1.2) followed by phosphate buffer (pH 6.8) as a two-step dissolution medium; sink conditions were maintained throughout the experiment. Experiments were conducted on Furosemide Oral Solution USP (Furoped®, SL Samrath, India) and all granule formulations at 37 ± 0.5 °C and 50 RPM agitation rate.

The experimental procedure involved a gastric condition for 1 hour with 100 mL, followed by intestinal conditions simulated using 200 mL for 3 hours. Samples were taken at 5, 15, 30, 45, 60, 75, 90, 120, 180, and 240 minutes. For each time point, 2 mL was withdrawn and replaced with fresh medium at the same temperature. The samples were filtered using 0.45 µm filters. UV spectroscopy at 273 nm in 0.1 N HCl and 277 nm in pH 6.8 phosphate buffer measured furosemide concentrations (Martir et al. 2020).

Disintegration test

Deionized water (9 mL) was used to flush the straw, and the time required to dissolve the granules inside the straw was recorded. The endpoint was reached when no granules remained within the straw (Király et al. 2022).

Evaluation of the best formula

The best formula was evaluated using differential scanning calorimetry (DSC) and Fourier transform infrared spectroscopy (FTIR).

Drug content

Six grams of the best formula were added to 100 mL of deionized water. The mixture was stirred for 30 minutes at 100 RPM using a magnetic stirrer. Measurements were taken by spectrophotometry at 276.5 nm after filtering through a 0.45 µm syringe filter and diluting with deionized water (Khalil et al. 2023).

Mass uniformity

Single-dose mass uniformity was tested using the European Pharmacopeia 10th edition weighing method. Twenty granules were randomly selected. Each was weighed using an electronic balance, and the mean weight was calculated (European Pharmacopoeia Commission 2019).

Impact of temperature and humidity on the optimum formula

An accelerated stability study was conducted by storing the best formulation (sealed in vials with screw caps) under harsh temperature and humidity conditions for three months. The vials were kept in an incubator and desiccator at 40 °C and 75% relative humidity (Tong et al. 2022; Muter and Habeeb 2025). A relative humidity of 75% was achieved using a desiccator containing saturated sodium chloride (S'Ari et al. 2021). The appearance and drug content of each sample were evaluated after one, two, and three months.

Statistical analysis

Analysis was performed using SPSS version 14 and GraphPad Prism 10.4. One-way ANOVA with post hoc Tukey test was applied to continuous variables. The p-value was considered significant if < 0.05.

Results and discussion

Percentage yield of the prepared ASD

Calculating the percentage yield of the prepared formula is crucial for assessing the effectiveness of the preparation procedure. The yield values from all the generated BASD formulas ranged from 92% to 99% (95%, 99%, and 92% in Formulas E, F, and G, respectively). A small loss occurred during some stages of the formula preparation or sieving process. The outcome demonstrated the compatibility of the solvent evaporation process with the chosen material for this preparation.

Drug content

The drug content of all formulations fell within the range of 96–99% w/w (98 ± 0.99%, 99.41 ± 0.61%, and 96.79 ± 0.29% in Formulas E, F, and G, respectively). This fulfills the specifications outlined by the United States Pharmacopeia (90–105%) (Pharmacopeia 2018), ensuring negligible furosemide loss during the preparation and confirming that drug particles are evenly distributed in all the produced formulations.

Differential scanning calorimetry

The DSC thermal analysis revealed a sharp melting endothermic peak of furosemide at 221 °C, which confirms the compound's identity, purity, and crystallinity based on previously reported data (Shariare et al. 2019; Diniz et al. 2020; Abu-Much et al. 2022). After solvent evaporation, furosemide exhibited its peak at 220 °C. The melting point of furosemide, both in its crystalline form and after solvent evaporation, was approximately 221 °C; this can be attributed to furosemide's transformation into another polymorph during the melting process. Furthermore, the solvent evaporation procedure did not produce a glass transition temperature (Tg) for furosemide, suggesting that the compound remained in a crystalline state (Sulaiman Hameed et al. 2022). Upon being mixed with PVP-K30 (Formula B), the physical mixture exhibited a melting peak at approximately 235 °C. However, after solvent evaporation (Formula F), the melting peak disappeared and a broad peak emerged at around 100 °C. This occurrence is likely attributed to the loss of water from PVP-K30. The absence of a melting peak suggests the formation of an ASD. The DSC analysis of gefitinib solid dispersion prepared by spray drying using PVP-K30 as a carrier exhibited a broad endothermic peak at 50 °C, indicating water loss in the sample due to PVP's high hygroscopicity; however, no melting point peak was observed (Mustafa et al. 2022). When combined with HPMC-E6, the physical mixture exhibited a melting peak at approximately 225 °C (Formula A). The DSC curve displayed an endothermic peak between 100 °C and 150 °C, attributed to surface water removal. Subsequently, decomposition occurred at this temperature. However, when the solvent was evaporated (Formula E), a broad endothermic event (Tg) often occurred concurrently with a reduced melting peak; this suggests that not all the drug transitioned to the amorphous state (partial amorphization) (Kim et al. 2021). When combined with Soluplus®, the melting point peak of furosemide was absent in both Formulas C and G. This indicates the existence of an interaction between crystalline furosemide and Soluplus® and the formation of uniform mixtures and full amorphization. Apixaban ASD showed similar results when prepared using Soluplus® (Lee et al. 2023), as seen in Fig. 2.

The physical mixture with these polymers may lead to the amorphization of furosemide. The polymers can inhibit crystallization, resulting in an amorphous state that does not exhibit distinct crystalline peaks in DSC thermograms. The polymers may interact with furosemide at a molecular level, disrupting its crystalline structure and promoting a more amorphous form. This interaction can prevent the formation of crystalline peaks in the thermograms. The melting temperatures (Tm) of the polymers used (PVP, HPMC, Soluplus®) are generally lower than that of furosemide. For example, PVP melts at approximately 150–180 °C, HPMC

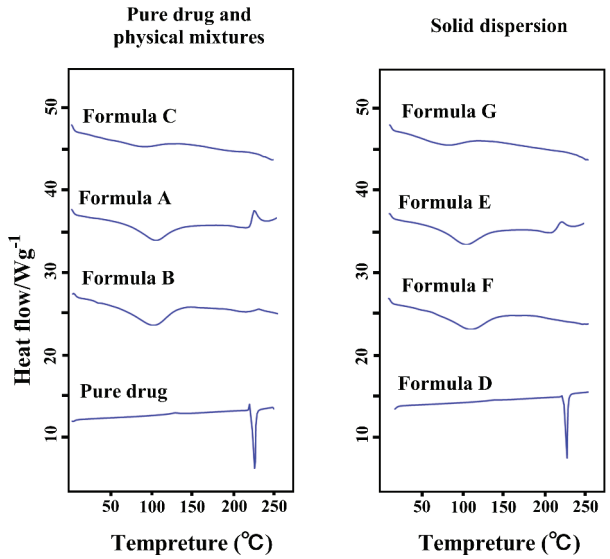

Figure 2. The DSC thermograms of various formulas.

at around 190–200 °C, and Soluplus® at 70–80 °C; these temperatures are lower than the melting temperature of furosemide, which is around 210–220 °C. As a result, the polymers can melt and form a homogeneous mixture with furosemide, leading to the absence of crystalline peaks in the DSC thermograms (Howatson 2012; Haynes 2016).

Powder X-ray diffraction

The P-XRD technique can be employed to evaluate alterations in the crystalline structure of a pharmaceutical compound that undergoes conversion into a solid dispersion and precipitates in an amorphous state. This transformation could enhance its solubility and confirm the findings of the DSC tests.

Fig. 3 shows the P-XRD of furosemide in various formulations. The drug's P-XRD patterns showed several peaks at 2θ angles of 6.01°, 12.09°, 18.13°, 18.17°, 22.1°, 24.81°, and 28.65°. These peaks, characterized by their strong Bragg reflections, confirm the crystalline structure of furosemide, which has been previously reported (La Rocca et al. 2022).

PVP and Soluplus® exhibited a halo pattern devoid of diffraction peaks, suggesting that the polymers utilized were in a non-crystalline condition (Jia et al. 2022; Saraf et al. 2022). The presence of distinct sharp peaks in the P-XRD pattern of HPMC-E6 at 2θ angles of 32.51°, 45.62°, and 56.44° indicates its semi-crystalline structure (Zhang et al. 2021). The furosemide physical mixtures with HPMC-E6, PVP-K30, and Soluplus® showed similar diffraction patterns, with a reduction in the number of peaks, which most likely indicates a drop in the drug's crystallinity. No new peaks or peak displacements were observed, suggesting that no new interactions occurred (dos Santos et al. 2021). The reduction of Bragg peaks observed during furosemide solvent evaporation suggests that the drug may lose crystallinity and revert to a semi-crystalline state, as previously observed in a study on azithromycin (Ismael et al. 2020).

The samples obtained by BASDs revealed a lower relative intensity of the furosemide peaks than the physical mixtures, indicating a loss of drug crystallinity in the BASDs.

In the case of BASD with PVP-K30 (Formula F), halo peaks were observed, which indicate full amorphization of furosemide due to molecular interaction with the carrier. The results confirmed that furosemide had been effectively distributed in PVP-K30 and transformed into an amorphous structure. This result is consistent with a previous study in which quercetin was prepared as an ASD with PVP-K30 (Febriyenti et al. 2020).

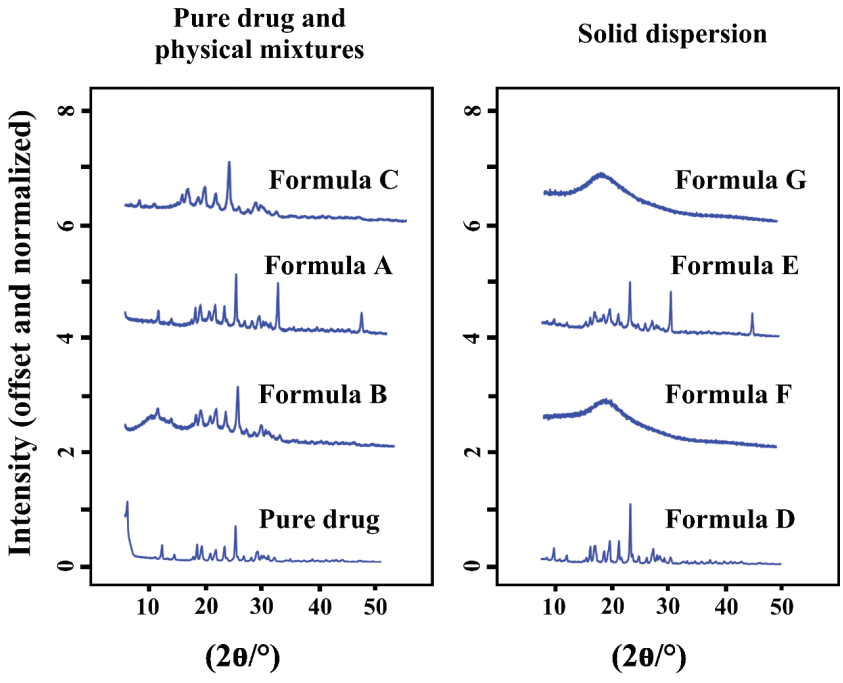

Figure 3. The PXRD patterns of various formulas.

In BASD with Soluplus® (Formula G), the absence of clearly defined crystalline peaks, replaced by a wide halo, indicates that the drug molecules are evenly distributed at the molecular level within the polymer, i.e., complete amorphization. This result agrees with a previously reported study (Vasconcelos et al. 2021).

On the other hand, the diffractogram of the furosemide–HPMC-E6 BASD exhibited prominent diffraction peaks, indicating the formulation's crystalline characteristics. The produced BASD exhibited distinct diffraction peaks at 2θ angles of 26.61°, 32.31°, and 47.1°, which confirm its crystalline structure. These findings suggest that the presence of HPMC-E6 and its intermolecular interactions—specifically bonding between the individual chains of the monomer—are responsible for the observed crystalline nature, leading to the formation of aggregates and a significant level of crystallinity (Ravikumar et al. 2022).

Overall, the results of the current study are consistent with those of DSC and P-XRD.

Fourier transform infrared spectroscopy

The FTIR spectra of pure furosemide powder exhibited distinctive absorption bands. Stretching peaks for furosemide were observed at 3396 and 3349 cm^{-1} for NH_2, 3280 cm^{-1} for NH, 1141 cm^{-1} for SO_2, and 1670 cm^{-1} for C=O, as shown in Table 4, Fig. 4. Several previous reports describe a spectral pattern similar to that of furosemide (Bezerra et al. 2021a; Li et al. 2021; Hossain et al. 2023; Alshora et al. 2024).

The FTIR spectra of Formulas A, B, and C (physical mixtures) and Formula E (BASD) showed negligible differences, as presented in Table 4, Fig. 4.

After solvent evaporation, the FTIR spectra of Formula F differed significantly from those of Formula B. The primary amine peaks shifted from 3396 and 3348 cm^{-1} to 3307 and 3089 cm^{-1}, respectively, while the furosemide NH_2 symmetric stretching and carbonyl peaks shifted from 3284 and 1678 cm^{-1} to 2956 and 1676 cm^{-1}, respectively. The stretching mode of S=O also shifted from 1141 to 1161 cm^{-1}, confirming that these functional groups interact with PVP. The shift in furosemide characteristic peaks suggests the presence of hydrogen bonding between the components of the BASD (furosemide and PVP-K30), as illustrated in Table 4, Fig. 4. These findings are consistent with previous studies involving resveratrol solid dispersions prepared using Eudragit® E PO, polyethylene glycol 6000, PVP-K30, and Soluplus®, in which peak shifts and broadening indicated hydrogen bond formation (Yu et al. 2023).

In Formula G, the peak of primary amine shifted from 3396 and 3348 cm^{-1} to 3317 and 3084 cm^{-1}. The aromatic $NHCH_2$ peak also shifted from 3282 to 2927 cm^{-1}, the carbonyl group spectrum grew from 1672 to 1683 cm^{-1}, and the sulfonyl group band increased from 1141 to 1163 cm^{-1}, compared to Formula C. The carbonyl group peak and the sulfonyl group peak exhibit a greater wavenumber (blue shift), suggesting that the carbonyl and sulfonyl groups of furosemide may participate in the creation of hydrogen bonding, as seen in Table 4, Fig. 4. Nandi et al.

Table 4. FTIR data of furosemide in all formulations containing furosemide.

Group (cm^{-1})	Pure drug	Formula D	Formula A	Formula E	Formula B	Formula F	Formula C	Formula G
SO_2NH_2	3396; 3349	3396; 3349	3396; 3348	3396; 3348	3396; 3348	3307; 3089	3396; 3348	3317; 3084
AR-$NHCH_2$	3280	3282	3282	3282	3284	2956	3282	2927
C=O	1670	1674	1670	1670	1678	1676	1672	1683
S=O	1141	1141	1141	1141	1141	1161	1141	1163

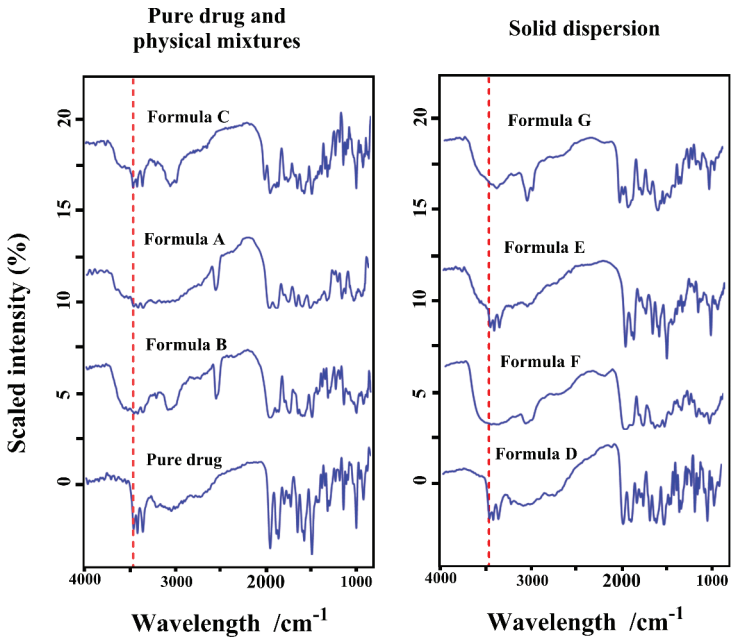

Figure 4. FTIR patterns of various formulas.

reported a similar observation in simvastatin/Soluplus® ASD using a single-step, organic solvent-free supercritical fluid process (Nandi et al. 2021).

Determination of saturated solubility

The solubility of furosemide in water and Tween 80 (0.1%) was found to be 0.09 mg/ml, consistent with the previous study (Diniz et al. 2020). Fig. 5 shows that all furosemide formulations were more soluble than the pure medication (p-value < 0.05) when saturated with water and 0.1% Tween 80. HPMC-E6 and PVP-K30 increased solubility 15-fold and 13.5-fold, respectively.

HPMC, in particular, contains hydrophilic hydroxypropyl groups and methyl groups, which are hydrophobic, resulting in a polymer with surface-active properties (Kayaert and Van den Mooter 2012). HPMC is useful in delaying the crystallization of amorphous forms of furosemide during dissolution (Alonzo et al. 2010); this explains the higher solubility of furosemide in the HPMC formulation (Formula E).

Polyvinylpyrrolidone (PVP) is frequently utilized as a polymer in amorphous solid dispersions (ASD) owing to its capacity to create a stable amorphous matrix with the examined pharmaceuticals (Yu et al. 2018); this can inhibit the medication from crystallizing, preserving it in a more soluble amorphous form (Budiman et al. 2022a, 2022b). The amorphous form of medicine typically demonstrates more solubility than its crystalline equivalent, perhaps enhancing dissolution and absorption in the gastrointestinal tract (Dengale et al. 2016). PVP serves as a carrier or matrix for the medication in the ASD, aiding in the preservation of the drug in a stable and amorphous state; this is especially advantageous for pharmaceuticals with limited water solubility (Wlodarski et al. 2018; Monschke and Wagner 2020). These properties of PVP explain the increase in furosemide solubility in Formula F.

Soluplus® is a graft copolymer (an amphiphilic polymer) consisting of polyethylene glycol (PEG), polyvinyl caprolactam, and polyvinyl acetate. Some of its components are hydrophilic, such as the strongly hydrated PEG segment, which increases its solubility, while other components are hydrophobic, including vinyl acetate and vinyl caprolactam. This complex relationship was associated with a slight increase in solubility in Formula G, but it was not as high as those seen in Formulas E and F (Alopaeus et al. 2019).

Hydrophilic carriers and drug particle adsorption on their surfaces may explain this action (Tung et al. 2021). The drug's solubility increased due to the reduced particle size and increased solvent–drug interfacial area compared to the pure drug; previous work supports this result (Malkawi et al. 2022).

In vitro dissolution studies

According to Fig. 6, about 45.80% of pure furosemide dissolves within 120 minutes. The physical mixture formulas based on HPMC-E6 and PVP-K30 (Formulas A and B) and all solid dispersion formulas (Formulas E, F, and G) released furosemide more effectively than the pure drug (p-value < 0.05). Meanwhile, the Soluplus® physical mixture formula showed a lower release profile than the pure drug.

Solvent evaporation improved the dissolving profile of furosemide (Formula D), resulting in 84.88% drug solubility after 120 minutes, which was significantly higher than the pure drug (p-value < 0.05). This enhanced solubility is attributed to amorphization and/or particle size reduction and surface area expansion.

The BASD formulas (Formulas E, F, and G) exhibited dissolution rates of 90.20%, 87.18%, and 79.96% at 120 minutes, respectively. The solid dispersion dissolving rates followed the descending order: Formula E > Formula F > Formula G. Their dissolution rates were 1.96, 1.9, and 1.7 times faster, respectively, than that of pure crystalline furosemide (p-value < 0.05), consistent with a previous study in which PVP-K17s/nisoldipine ASDs increased drug release after 120 minutes (Chavan et al. 2020).

The BASD containing HPMC-E6 dissolved faster than that with PVP-K30. The crystal inhibition property of HPMC facilitates dissolution in the E6-based dispersion. HPMC-E6 dissolves more rapidly than PVP because it inhibits precipitation more effectively (Ishtiaq et al. 2022).

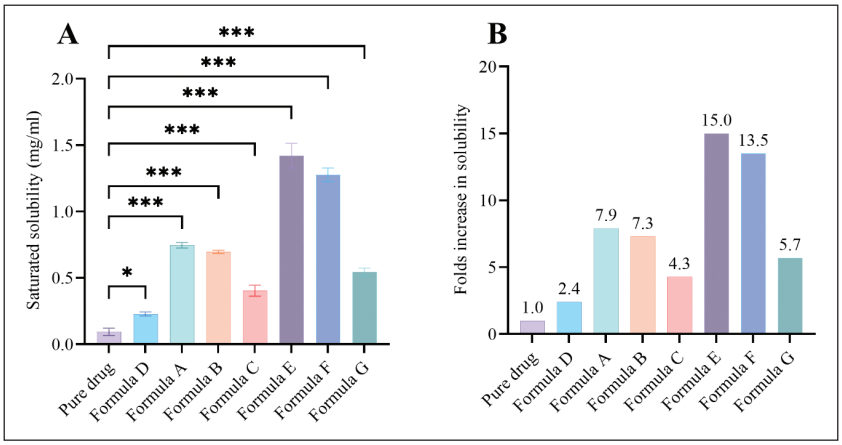

Figure 5. Saturated solubility study of furosemide. **A.** Absolute solubility; **B.** Fold increase in solubility compared to pure drug. One-way ANOVA with post hoc Tukey test; data presented as mean ± standard deviation.

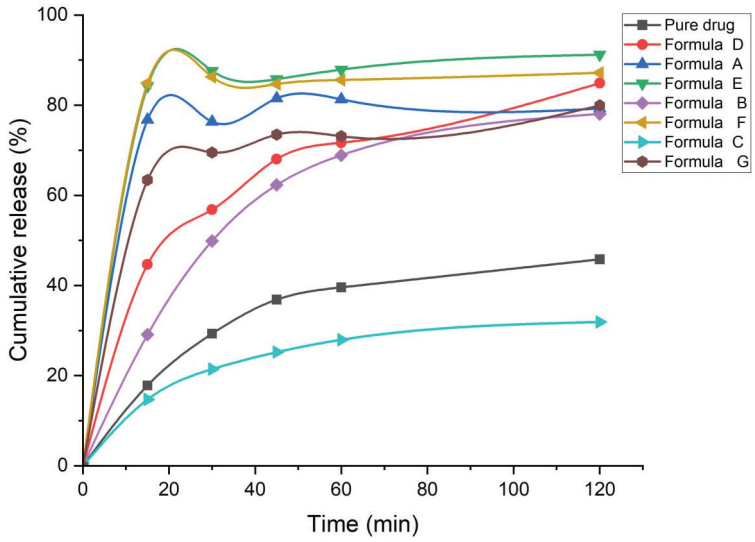

Figure 6. Dissolution profile of various formulas.

Multiple mechanisms in Soluplus® also accelerate furosemide dissolution in solid dispersions. Soluplus®, an amphiphilic polymer, prevents crystal formation and enhances molecular dispersion of furosemide in its amorphous state. This increases surface area and wettability, thereby speeding up aqueous dissolution—consistent with previous findings (Vasconcelos et al. 2021).

Selection of the best BASD formula

The preferred formulation is the PVP-K30 solid dispersion (Formula F) due to its advantageous results in DSC, XRPD, and FTIR investigations. The rationale behind selecting Formula F is the conclusive evidence provided by various analytical techniques, demonstrating that the formula is an amorphous system with improved solubility.

Field emission-scanning electron microscopy (FESEM)

Fig. 7 shows the surface properties of furosemide in its pure form and in various formulations. In contrast to pure furosemide (Fig. 7A), which exhibited a rod-shaped, needle-like crystal structure, Formula F (Fig. 7B) displayed a layered, flaky structure with sharp edges and no crystalline features. Complexation with PVP-K30 results in polymorphic variations in crystal habit and transformation to an amorphous state, suggesting the successful production of an ASD.

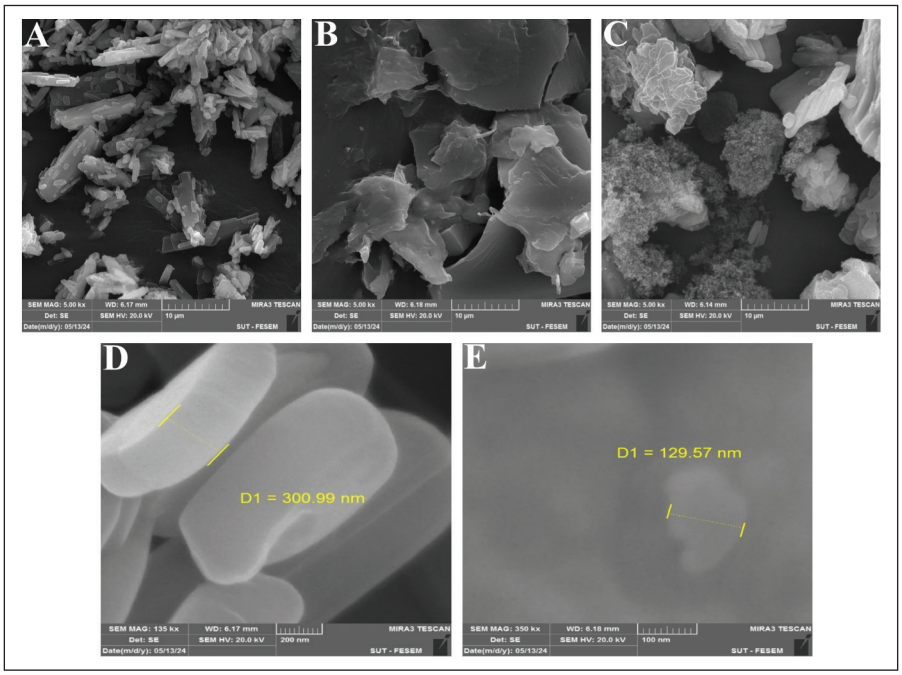

Figure 7. FESEM images of various furosemide formulas in the pre-formulation phase of the study. **A.** Pure furosemide; **B.** Formula F; **C.** Formula B; **D.** Pure furosemide at higher magnification, and **E.** Formula F at higher magnification.

Fig. 7C shows a physical mixture of spherical excipients and a smooth, layered solid dispersion, supported by Zhou et al.'s solvent evaporation investigation, which increased luteolin solubility in a PVP solid dispersion (Zhou et al. 2022).

The solvent evaporation process produces particles with a narrow size distribution due to a high surface area-to-volume ratio. Fig. 7D shows that raw furosemide particles had a mean diameter of 300.99 nm. The formulated BASD (Fig. 7E) further reduced drug particle size to 129.57 nm and altered the furosemide structure, resulting in a distinct and consistent morphology. Particle size reduction and changes in particle appearance indicate the effectiveness of the solvent evaporation method (Shah et al. 2024).

Granules evaluation

Angle of repose

Table 5 presents the angle of repose values for all granule formulations. According to the European Pharmacopoeia, flow properties improve with a lower angle of repose, and values between 25° and 35° are generally considered indicative of good flowability (Buanz 2021). The evaluated formulations demonstrated good to excellent flow characteristics. Notably, granules of Formulation F9 had a lower angle of repose (22.58°) than those of Formulation F1 (31.59°), indicating superior flow properties.

Talc (TLC) affects formulations containing crospovidone and Aerosil® super disintegrants. TLC reduces granule friction and cohesive interactions, thereby lowering the angle of repose (Apeji et al. 2022). The angle of repose further decreased in formulations as the crospovidone content increased from 2.5% to 5%. Moreover, the inclusion of Aerosil® in the formulations reduced both the angle of repose and compressibility, confirming that Aerosil® enhances the flowability of furosemide powder. The flowability enhancement process involves the physical separation of host particles caused by the presence of guest particles adhering to their surface, which leads to a reduction in cohesion. When interparticle cohesiveness is sufficiently diminished, gravitational forces predominate over cohesive forces, markedly improving powder flow (Tadauchi et al. 2022).

Bulk density and tapped density

Formulas F7, F8, F9, and F10, which contain Aerosil®, exhibited higher bulk and tapped densities than the other formulations, attributable to Aerosil®'s superior flow-enhancing properties. Table 5 presents the bulk and tapped density values for each granule formulation based on density measurements.

Compressibility index (Carr's index) CI and Hausner's ratio (HR)

The Carr's index quantifies powder bridge strength and stability, while the Hausner ratio evaluates particle friction. Carr's index is low when bulk and tapped density are similar, indicating high granule flowability. However, granules with poor flow have high Carr's index values, indicating significant variations in bulk density. CI and HR flowability matched the angle of repose. These results show that crospovidone and Aerosil® granules flow better than pullulan polysaccharides. Flow properties are good, with 5–15% compressibility index values. Table 5 shows Hausner's ratio and Carr's index results. All granule formulations were measured within acceptable flow characteristics following the European Pharmacopoeia (Buanz 2021).

In vitro dissolution study

A) In water.

This study aims to predict formulation behavior in straws during water intake. The dissolution data for furosemide are presented in Fig. 8. All of these formulations exhibited a relatively short drug release time of 1 minute, as the amount of released furosemide did not exceed 30.98%.

B) In two dissolution steps.

Fig. 9 shows the dissolution rate at different pH values. The drug release percentage of formulas was initially assessed in HCl buffer at pH 1.2, which mimics stomach acidity, and furosemide dissolves more slowly. The results indicated a relatively lower drug release percentage than Furosemide Oral Solution USP (Furoped®, SL Samrath, India), reaching approximately 50.81% within 60 minutes in F9.

Table 5. Angle of repose, bulk density, tapped density, Carr's index, Hausner's ratio, and disintegration time values for each granule formulation.

Formula	Angle of repose	Type of flow	Bulk density	Tapped density	Carr's index	Hausner's ratio	Type of flow	Disintegration time (sec)
F1	31.59	Good	0.45 ± 0.15	0.51 ± 0.14	25%	1.33	Passable	65
F2	32	Good	0.45 ± 0.12	0.51 ± 0.16	22%	1.28	Passable	53
F3	30.8	Very good	0.46 ± 0.15	0.52 ± 0.12	20%	1.25	Fair	24
F4	29.72	Very good	0.45 ± 0.13	0.56 ± 0.12	20%	1.25	Fair	35
F5	28.05	Very good	0.45 ± 0.15	0.56 ± 0.15	15%	1.17	Good	22
F6	28.05	Very good	0.46 ± 0.20	0.57 ± 0.15	15%	1.17	Good	27
F7	24.18	Excellent	0.49 ± 0.20	0.58 ± 0.12	15%	1.17	Good	13
F8	27.2	Very good	0.49 ± 0.11	0.58 ± 0.13	15%	1.17	Good	16
F9	22.58	Excellent	0.51 ± 0.10	0.59 ± 0.11	11%	1.12	Good	5-6
F10	23.02	Excellent	0.51 ± 0.13	0.59 ± 0.11	12%	1.13	Good	10

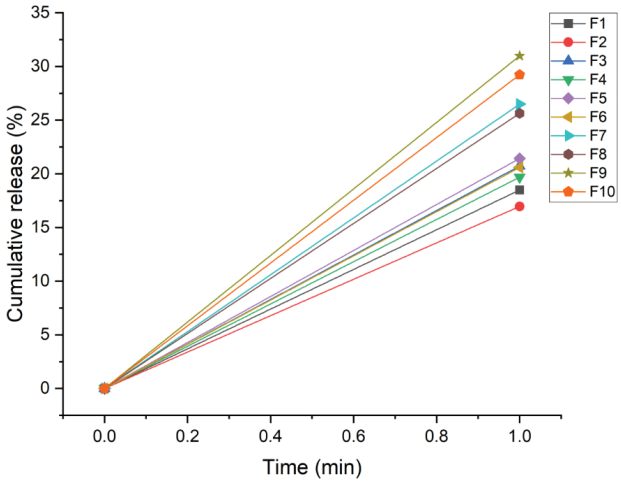

Figure 8. Dissolution profile of furosemide granule formulas in water at 37 °C.

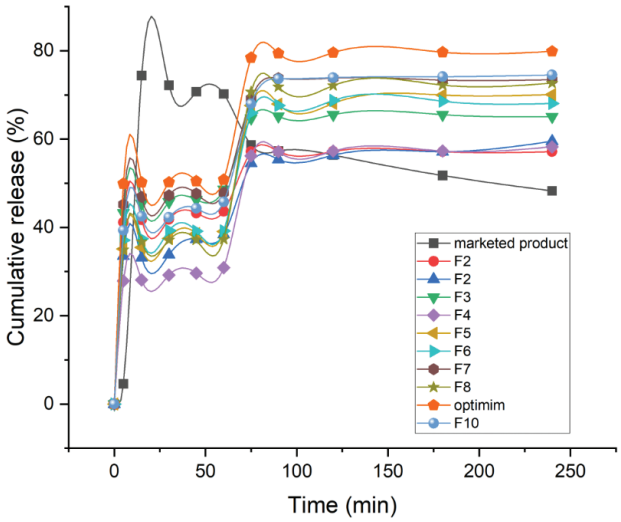

Figure 9. Dissolution profile of furosemide granule formulas in 0.1N HCl (pH 1.2) and phosphate buffer (pH 6.8) at 37 °C.

The lower solubility of furosemide in acidic environments may explain this. The drug dissolves more slowly in acidic conditions due to its pH-dependent solubility. Nevertheless, furosemide dissolves faster at pH 6.8 due to its higher solubility in nearly neutral or slightly alkaline conditions.

Drug release is faster (p-value < 0.05) with crospovidone (F3 to F6) than with pullulan polysaccharides (F1 and F2), with a maximum of 59.48% in 4 hours for F2; it is clearly shown that the percentage of drug release is influenced by both the type and quantity of the super disintegrant agent employed. Crospovidone's rapid water absorption and swelling facilitate the dissolution of the drug more effectively than pullulan polysaccharides. This rapid breakdown accelerates drug release (Bezerra et al. 2021a).

In formulations F7 to F10, the addition of Aerosil as a super disintegrant speeds dissolution (p-value < 0.05). Aerosil enhances granule wetting and dispersion, improving dissolution (Alam et al. 2024). Aerosil's glidant properties enhance powder flow and dispersion, thereby accelerating drug release. Additionally, increased superdisintegrant levels in formulations could enhance drug release. Increased super disintegrants cause rapid granule disintegration and drug solubility due to substantial swelling.

Formulations with sodium bicarbonate release furosemide faster (p-value < 0.05) than those with calcium carbonate. When in contact with water, sodium bicarbonate acts as a release enhancer by creating carbon dioxide gas. This gas disintegrates and dissolves quickly due to internal pressure (Mahmoud et al. 2023).

Thus, the pH of the dissolving medium, type of super disintegrant, concentration, and release enhancers all affect furosemide dissolution profiles. Excipient selection is crucial during formulation development to achieve the desired drug release characteristics. Based on the findings of this investigation, formulation F9 exhibited the highest percentage of furosemide release. This formulation contained 5% crospovidone, 1% Aerosil®, and 1% sodium bicarbonate and achieved a drug release rate of 79.86% within 4 hours. This type of release is similar to Guimarães et al.'s work, which studied dissolution tests on Singulair® granules and chewable tablets (Guimarães et al. 2022).

Disintegration time test

Table 5 shows that granule disintegration time was a crucial parameter that varied between formulas. The disintegration time was determined by measuring the duration for the granules to break down completely; this was confirmed by observing a change in the color of the resulting solution and the absence of any solid particles. Formula F9 disintegrated fastest (5–6 seconds) (p-value < 0.05) due to its 5% crospovidone and 1% Aerosil® superdisintegrants.

The concentration of superdisintegrants plays a crucial role in the disintegration process. Higher concentrations of superdisintegrants typically lead to a more pronounced and rapid swelling action, decreasing the disintegration time; this can explain why formulations with increased concentrations of crospovidone showed reduced disintegration time (Berardi et al. 2021). Crospovidone is known for its high capillary activity and pronounced hydration capacity, which enables it to absorb water and swell rapidly. This rapid swelling action disrupts the granule structure quickly, leading to faster disintegration (Sutthapitaksakul et al. 2022). In addition, using crospovidone as the only disintegrant did not yield the desired disintegration qualities of the granules (Purandare et al. 2024). Therefore, the presence of Aerosil® can enhance the disintegration process by improving the flow properties and uniform distribution of granules, thus facilitating quicker access of water to the superdisintegrant.

Additionally, Aerosil® can act as a glidant, reducing inter-particulate friction and aiding in the rapid breakdown of granules. Sodium bicarbonate acts as an effervescent agent, releasing carbon dioxide gas upon contact with water. This gas formation creates internal pressure within the granules, aiding in their rapid breakup. The effervescent action of sodium bicarbonate accelerates disintegration, especially when used with superdisintegrants like crospovidone and Aerosil®.

Selection of the best furosemide formula

From the above formulas' characterization and evaluation results, formula F9 was selected as the best formula compared with the marketed product. It exhibits a faster disintegration time of 5–6 seconds, good flowability properties, and drug release from formula F9, which was found to have 50% release within 1 hour in acidic media (pH 1.2) and 79% at 4 hours in phosphate buffer (pH 6.8). Therefore, formula F9 was selected as the best formula.

Evaluation of the best formula (F9)

Drug content

The drug content in formula F9 was 95.42% ± 1.24. The allowable drug content fluctuation range is 85–115%; this meets the 10th edition of the European Pharmacopoeia's single-dose formulation standards (European Pharmacopoeia Commission 2019).

Mass uniformity

In the European Pharmacopoeia 10th edition, the 10% variation limit was met; only two individuals differed from the average mass by a percentage, and none by more than twice that of the individual's percentage deviation, which ranged from 3.75 to 7.5%, suggesting that formula F9 demonstrated a high degree of mass uniformity (European Pharmacopoeia Commission 2019).

Differential scanning calorimetry

Fig. 10A compares DSC images of the best furosemide granules (Formula F9) and pure furosemide. Furosemide's melting point and medication degradation cause an endothermic peak of about 221 °C. The drug's endothermic peak was absent from furosemide granules in Formula F9 DSC images due to furosemide solubility and homogeneous distribution in the melting polymers. The absence of the furosemide endothermic peak also shows that the granules of furosemide are thermally stable. This finding aligns with a prior investigation (Alshora et al. 2024).

Fourier transform infrared spectroscopy

As seen in Fig. 10B, the FTIR spectra of Formulation F9 granules were compared to those of the physical mixture. The physical mixture was characterized by furosemide stretching peaks at 3396 and 3348 cm^{-1} for NH_2, 3284 cm^{-1} for NH, 1141 cm^{-1} for SO_2, and 1678 cm^{-1} for C=O. The FTIR spectra of the best formula exhibit distinct peaks at 3398 and 3346 cm^{-1} for NH_2, 3288 cm^{-1} for NH, 1151 cm^{-1} for SO_2, and 1668 cm^{-1} for C=O.

The absence of any additional peaks and the presence of all drug peaks in Formula F9 suggest no interaction with the excipient. This indicates the excipient's compatibility with furosemide, ensuring that there were no chemical interactions or degradation of furosemide during the preparation of the granules.

This investigation was correlated with a previous study, which examined the synthesis and characterization of furosemide-loaded sericin/alginate beads. The study found that the furosemide-loaded formulations and pure furosemide spectra showed similarity, indicating the drug was compatible with the sericin/alginate blend (Bezerra et al. 2021b).

Field emission-scanning electron microscopy

Fig. 11 shows that furosemide granules have better surface characteristics and a densely packed, spherical configuration that facilitates smooth mobility. Formula F9 had 61.69 nm particles, while the particle size of the pure drug was 300.99 nm. This finding resembles ibuprofen co-crystal granules prepared via fluidized bed granulation (Todaro and Healy 2021).

Impact of temperature and humidity on the best formula

Crystalline furosemide presents significant challenges for the pharmaceutical industry due to its inadequate solubility. Moreover, furosemide is recognized for its instability under harsh storage conditions. It experiences acid-catalyzed hydrolysis in aqueous solutions, photochemical degradation in the solid phase, and thermal disintegration at its melting point. Consequently, crystalline furosemide appears to be highly susceptible to deterioration under unsuitable storage or manufacturing settings (Adrjanowicz et al. 2011).

Formula F9 was sealed in a container and accelerated at 40 °C and 75% relative humidity for three months. During storage, it remained similar in appearance (Fig. 12). The initial drug content of Formula F9 was 95.42% ± 1.24%, and after one, two, and three months of storage, it became 95.31% ± 1.2, 94.20% ± 0.9, and 93.64% ± 1.3%, respectively. The stability data showed that furosemide and

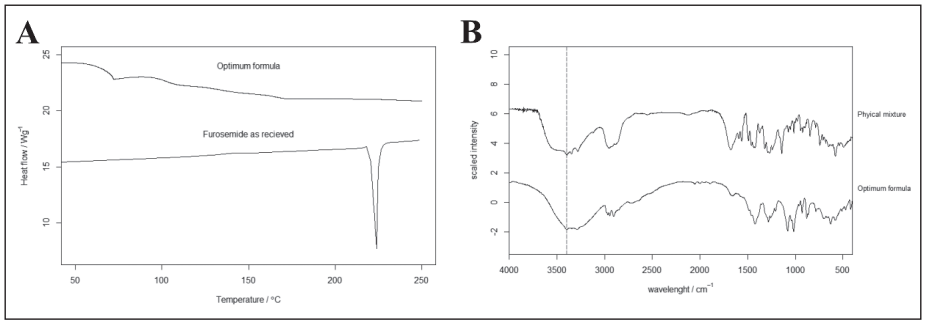

Figure 10. Assessment of pure furosemide and Formula F9 utilizing. **A.** DSC thermograms and **B.** FTIR patterns.

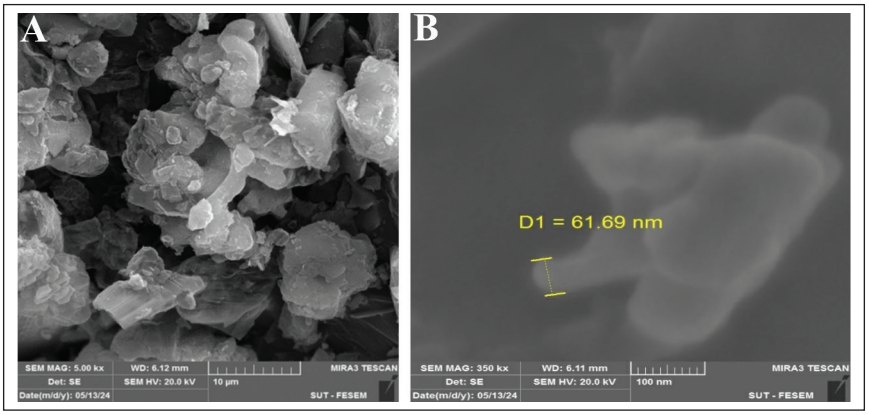

Figure 11. FESEM images of furosemide granules (Formula F9). **A.** Shape of granules; **B.** Particle size of granules.

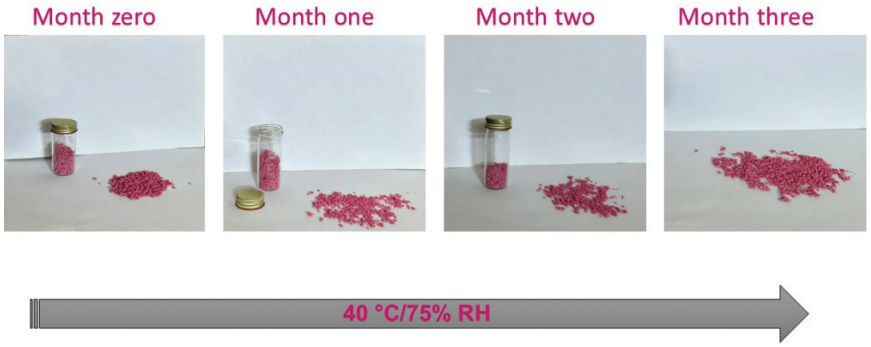

Figure 12. Stability test: the physical appearance of granules (Formula F9).

PVP-K30 drug-polymer interactions encapsulated the amorphous drug, improving its solubility and stability. Due to the robustness and adaptability of the solid dispersion system, furosemide with PVP solid dispersion granules showed no significant changes in appearance or drug content after a 3-month stability trial under extreme conditions. This finding aligns with another study on the stability of hot-melt extruded telmisartan solid dispersions over 1 month. The samples did not degrade under accelerated stability conditions of 40 °C/75% relative humidity, and there was no substantial decrease in drug content; it was approximately equivalent to that at the initial time (Almotairy et al. 2021).

However, while these findings suggest that the formulation is robust under accelerated conditions, the slight gradual decrease in drug content leaves open the possibility that, over extended periods or under less controlled ambient conditions, furosemide might eventually exhibit instability. In essence, the accelerated study provides encouraging evidence for the short- to mid-term stability required for pediatric formulations. Still, it also underscores the importance of long-term stability assessments under real-world storage conditions to confirm the shelf life and ensure consistent therapeutic efficacy.

Conclusion

This work produced binary solid dispersion formulations of furosemide with improved solubility. The presence of PVP-K30 in the solvent-evaporated product creates a completely amorphous solid dispersed system, which enhances the drug dissolution rate due to its miscible nature. This information can be utilized in future endeavors to alter furosemide's physical characteristics and dissolution rate. In light of this study, the granule formulations containing 12 mg of furosemide were formulated in straws with ultrafast disintegration time. It was found that F9 formulations (containing 5% crospovidone, 1% Aerosil®, and 1% sodium bicarbonate) have the best properties. Overall, the developed granule formulations, filled into pediatric-friendly dosing devices, can potentially improve compliance and treatment outcomes for children.

Acknowledgements

The authors are extremely grateful to the participants of the study and the College of Pharmacy, Mustansiriyah University, for all their support.

Additional information

Conflict of interest

The authors have declared that no competing interests exist.

Ethical statements

The authors declared that no clinical trials were used in the present study.

The authors declared that no experiments on humans or human tissues were performed for the present study.

The authors declared that no informed consent was obtained from the humans, donors or donors' representatives participating in the study.

The authors declared that no experiments on animals were performed for the present study.

The authors declared that no commercially available immortalised human and animal cell lines were used in the present study.

Use of AI

No use of AI was reported.

Funding

No funding was reported.

Author contributions

Conceptualization, investigation, and manuscript preparation: Mohammed-Kadhum MF and Hameed GS. Supervision: Hameed GS. Statistical analysis and review of final results: Mohammed-Kadhum MF. Manuscript review and editing: Mohammed-Kadhum MF and Hameed GS. All authors have read and agreed to the published version of the manuscript.

Data availability

Data available upon request from the corresponding author.

References

Abraham S, Rameshkumar R, Chidambaram M, Soundravally R, Subramani S, Bhowmick R, Sheriff A, Maulik K, Mahadevan S (2021) Trial of furosemide to prevent acute kidney injury in critically Ill children: A Double-Blind, Randomized, Controlled Trial. Indian J Pediatr 88: 1099–1106. https://doi.org/10.1007/s12098-021-03727-3

Abu-Much A, Darawshi R, Dawud H, Kasem H, Abu Ammar A (2022) Preparation and characterization of flexible furosemide-loaded biodegradable microneedles for intradermal drug delivery. Biomater Sci 10: 6486–6499. https://doi.org/10.1039/D2BM01143C

Adrjanowicz K, Kaminski K, Grzybowska K, Hawelek L, Paluch M, Gruszka I, Zakowiecki D, Sawicki W, Lepek P, Kamysz W, Guzik L (2011) Effect of cryogrinding on chemical stability of the sparingly water-soluble drug furosemide. Pharmaceutical Research 28: 3220–3236. https://doi.org/10.1007/s11095-011-0496-4

Ainurofiq A, Putro DS, Ramadhani DA, Putra GM, Do Espirito Santo LDC (2021) A review on solubility enhancement methods for poorly water-soluble drugs. Journal of Reports in Pharmaceutical Sciences 10: 137–147. https://doi.org/10.4103/jrptps.JRPTPS_134_19

Akram A, Irfan M, Abualsunun WA, Bukhary DM, Alissa M (2022) How to improve solubility and dissolution of irbesartan by fabricating ternary solid dispersions: optimization and in-vitro characterization. Pharmaceutics 14(11): 2264. https://doi.org/10.3390/pharmaceutics14112264

Al-Hassani HR, Al-Khedairy EB (2021) Formulation and in-vitro evaluation of meloxicam solid dispersion using natural polymers. Iraqi Journal of Pharmaceutical Sciences 30: 169–178. https://doi.org/10.31351/vol30iss1pp169-178

Alam IZ, Sultana J, Kazi M, Uddin MN, Rahman MBM (2024) In vitro profiling of gliclazide-loaded aerosil 380 solid dispersion–based tablets with co-processed excipients. Journal of Pharmaceutical Innovation 19: 17. https://doi.org/10.1007/s12247-024-09817-x

Aldahhan ES, Radhi AAJIJoPS (2020) Co-amorphous system: a promising strategy for delivering poorly water-soluble drugs. Iraqi Journal of Pharmaceutical Sciences 29: 1–11. https://doi.org/10.31351/vol29iss1pp1-11

Almotairy A, Almutairi M, Althobaiti A, Alyahya M, Sarabu S, Alzahrani A, Zhang F, Bandari S, Repka MA (2021) Effect of pH Modifiers on the Solubility, Dissolution Rate, and Stability of Telmisartan Solid Dispersions Produced by Hot-melt Extrusion Technology. J Drug Deliv Sci Technol 65: 102674. https://doi.org/10.1016/j.jddst.2021.102674

Alonzo DE, Zhang GGZ, Zhou D, Gao Y, Taylor LS (2010) Understanding the behavior of amorphous pharmaceutical systems during dissolution. Pharmaceutical Research 27: 608–618. https://doi.org/10.1007/s11095-009-0021-1

Alopaeus JF, Hagesæther E, Tho I (2019) Micellisation mechanism and behaviour of soluplus®–furosemide micelles: Preformulation studies of an oral nanocarrier-based system. Pharmaceuticals 12: 15. https://doi.org/10.3390/ph12010015

Alshora D, Alyousef W, Ibrahim M (2024) Effects of functional biomaterials on the attributes of orally disintegrating tablets loaded with furosemide nanoparticles: In vitro and in vivo evaluations. J Funct Biomater 15: 161. https://doi.org/10.3390/jfb15060161

Alwan ZS, Ibrahim MA (2021) Study the effect of disintegrant types on preparation and in vitro evaluation of salbutamol sulfate effervescent granules. Kerbala J Pharm Sci 1: 1-9.

Alwossabi AM, Elamin ES, Ahmed EMM, Abdelrahman M (2022) Solubility enhancement of some poorly soluble drugs by solid dispersion using Ziziphus spina-christi gum polymer. Saudi Pharm J 30: 711–725. https://doi.org/10.1016/j.jsps.2022.04.002

Apeji YE, Ariko NA, Olayemi OJ, Olowosulu AK, Oyi AR (2022) Optimization of the extragranular excipient composition of paracetamol tablet formulation using the quality by design approach. Brazilian Journal of Pharmaceutical Sciences 58: e20544. https://doi.org/10.1590/s2175-97902022e20544

Aziz MS, Sabar MHJP (2025) Development and opti of an innovative raft-forming antiemetic gastro-retentive system. Pharmacia 72: 1–14. https://doi.org/10.3897/pharmacia.72.e147836

Babu NJ, Nangia A (2011) Solubility advantage of amorphous drugs and pharmaceutical cocrystals. Crystal Growth and Design 11: 2662–2679. https://doi.org/10.1021/cg200492w

Benet LZ, Broccatelli F, Oprea TI (2011) BDDCS applied to over 900 drugs. AAPS Journal 13: 519–547. https://doi.org/10.1208/s12248-011-9290-9

Berardi A, Bisharat L, Quodbach J, Abdel Rahim S, Perinelli DR, Cespi M (2021) Advancing the understanding of the tablet disintegration phenomenon – An update on recent studies. International Journal of Pharmaceutics 598: 120390. https://doi.org/10.1016/j.ijpharm.2021.120390

Bezerra IC, Moma MS, Freitas ED, Silva MG, Vieira MG (2021a) Development of a modified drug delivery system through the incorporation of furosemide into sericin and alginate matrix using the experimental design approach. Journal of Chemical Technology & Biotechnology 96: 650–661. https://doi.org/10.1002/jctb.6578

Bezerra ICS, de Freitas ED, da Silva MGC, Vieira MGA (2021b) Synthesis and characterization of furosemide-loaded sericin/alginate beads subjected to thermal or chemical cross-linking for delayed and sustained release. Polymers for Advanced Technologies 32: 461–473. https://doi.org/10.1002/pat.5099

Biegus J, Zymliński R, Testani J, Fudim M, Cox ZL, Guzik M, Iwanek G, Hurkacz M, Raj D, Marciniak D, Ponikowska B, Ponikowski P (2023) The blunted loop diuretic response in acute heart failure is driven by reduced tubular responsiveness rather than insufficient tubular delivery. The role of furosemide urine excretion on diuretic and natriuretic response in acute heart failure. Eur J Heart Fail 25: 1323–1333. https://doi.org/10.1002/ejhf.2852

Bindhani S, Mohapatra S (2018) Recent approaches of solid dispersion: A new concept toward oral bioavailability. Asian Journal of Pharmaceutical and Clinical Research 11: 72–78. https://doi.org/10.22159/ajpcr.2018.v11i2.23161

Brough C, Williams Iii RO (2013) Amorphous solid dispersions and nano-crystal technologies for poorly water-soluble drug delivery. International Journal of Pharmaceutics 453: 157–166. https://doi.org/10.1016/j.ijpharm.2013.05.061

Buanz A (2021) Powder characterization. In: Remington. Elsevier, 295–305. https://doi.org/10.1016/B978-0-12-820007-0.00016-7

Budiman A, Citraloka ZG, Muchtaridi M, Sriwidodo S, Aulifa DL, Rusdin A (2022a) Inhibition of crystal nucleation and growth in aqueous drug solutions: Impact of different polymers on the supersaturation profiles of amorphous drugs-the case of alpha-mangostin. Pharmaceutics 14(11): 2386. https://doi.org/10.3390/pharmaceutics14112386

Budiman A, Nurfadilah N, Muchtaridi M, Sriwidodo S, Aulifa DL, Rusdin A (2022b) The impact of water-soluble chitosan on the inhibition of crystal nucleation of alpha-mangostin from supersaturated solutions. Polymers (Basel) 14(20): 4370. https://doi.org/10.3390/polym14204370

Butreddy A, Almutairi M, Komanduri N, Bandari S, Zhang F, Repka MA (2021) Multicomponent crystalline solid forms of aripiprazole produced via hot melt extrusion techniques: An exploratory study. J Drug Deliv Sci Technol 63: 102529. https://doi.org/10.1016/j.jddst.2021.102529

Chavan RB, Lodagekar A, Yadav B, Shastri NR (2020) Amorphous solid dispersion of nisoldipine by solvent evaporation technique: preparation, characterization, in vitro, in vivo evaluation, and scale up feasibility study. Drug Delivery and Translational Research 10: 903–918. https://doi.org/10.1007/s13346-020-00775-8

Cram A, Breitkreutz J, Desset-Brèthes S, Nunn T, Tuleu C (2009) Challenges of developing palatable oral paediatric formulations. Int J Pharm 365: 1–3. https://doi.org/10.1016/j.ijpharm.2008.09.015

Dalal L, Allaf AW, El-Zein H (2021) Formulation and in vitro evaluation of self-nanoemulsifying liquisolid tablets of furosemide. Sci Rep 11: 1315. https://doi.org/10.1038/s41598-020-79940-5

Dengale SJ, Grohganz H, Rades T, Löbmann K (2016) Recent advances in co-amorphous drug formulations. Adv Drug Deliv Rev 100: 116–125. https://doi.org/10.1016/j.addr.2015.12.009

Diniz LF, Carvalho PS, Pena SAC, Gonçalves JE, Souza MAC, de Souza Filho JD, Bomfim Filho LFO, Franco CHJ, Diniz R, Fernandes C (2020) Enhancing the solubility and permeability of the diuretic drug furosemide via multicomponent crystal forms. International Journal of Pharmaceutics 587: 119694. https://doi.org/10.1016/j.ijpharm.2020.119694

Divya K, Vamshi G, Vijaykumar T, Rani M, Kishore B (2020) Review on introduction to effervescent tablets and granules. Kenkyu J Pharmacol 6: 1–9.

dos Santos KM, de Melo Barbosa R, Meirelles L, Vargas FGA, da Silva Lins AC, Camara CA, Aragão CFS, de Lima Moura TF, Raffin FN (2021) Solid dispersion of β-lapachone in PVP K30 and PEG 6000 by spray drying technique. Journal of Thermal Analysis and Calorimetry 146: 2523–2532. https://doi.org/10.1007/s10973-020-10473-9

Eid PS, Ibrahim DA, Zayan AH, Elrahman MMA, Shehata MAA, Kandil H, Abouibrahim MA, Duy LM, Shinkar A, Elfaituri MK, Minh LHN, Fahmy MM, Tam DNH, Vuong NL, Shah J, Do VBD, Hirayama K, Huy NT (2021) Comparative effects of furosemide and other diuretics in the treatment of heart failure: a systematic review and combined meta-analysis of randomized controlled trials. Heart Fail Rev 26: 127–136. https://doi.org/10.1007/s10741-020-10003-7

European Pharmacopoeia Commission (2019) European Pharmacopoeia, 10th edn. European Pharmacopoeia Commission: Strasbourg, France. Disintegration of Tablets and Capsules. European Pharmacopoeia Commission, 323–339.

Fadda HM, Weiler H, Carvalho M, Lee YZ, Dassouki H, AbuBlan R, Iurian S, Hamid A, Şeremet G, Li Z, Tuleu C, Minghetti P, Pauletti GM (2024) Pediatric oral extemporaneous preparations and practices: International Pharmaceutical Federation (FIP) global study. European Journal of Pharmaceutics and Biopharmaceutics 204: 114483. https://doi.org/10.1016/j.ejpb.2024.114483

Febriyenti PI, Zaini E, Ismed F, Lucida H (2020) Preparation and characterization of quercetin-polyvinylpyrrolidone K-30 spray dried solid dispersion. Journal of Pharmacy & Pharmacognosy Research 8: 127–134.

Guimarães M, Somville P, Vertzoni M, Fotaki N (2022) Performance Evaluation of Montelukast Pediatric Formulations: Part I—Age-Related In Vitro Conditions. The AAPS Journal 24: 26. https://doi.org/10.1208/s12248-021-00661-2

Gulsun T, Borna SE, Vural I, Sahin S (2018) Preparation and characterization of furosemide nanosuspensions. Journal of Drug Delivery Science and Technology 45: 93–100. https://doi.org/10.1016/j.jddst.2018.03.005

Hatem AQ, Ali WK (2023) Preparation and Characterization of Carvedilol Solid Dispersion by Kneading Method. Al Mustansiriyah Journal of Pharmaceutical Sciences 23: 367–377. https://doi.org/10.32947/ajps.v23i4.1092

Haynes WM (2016) CRC handbook of chemistry and physics. CRC press, 2670 pp. https://doi.org/10.1201/9781315380476

Hossain MS, Khaleque MA, Ali MR, Bacchu MS, Hossain MI, Aly Saad Aly M, Khan MZH (2023) Poly(3,4-ethylenedioxythiophene): Polystyrene sulfonate-modified electrode for the detection of furosemide in pharmaceutical products. ACS Omega 8: 16851–16858. https://doi.org/10.1021/acsomega.3c00463

Howatson AM (2012) Engineering tables and data. Springer Science & Business Media.

Ikeda Y, Ishii S, Maemura K, Oki T, Yazaki M, Fujita T, Nabeta T, Maekawa E, Koitabashi T, Ako J (2021) Association between intestinal oedema and oral loop diuretic resistance in hospitalized patients with acute heart failure. ESC Heart Failure 8: 4067–4076. https://doi.org/10.1002/ehf2.13525

Ishtiaq M, Asghar S, Khan IU, Iqbal MS, Khalid SH (2022) Development of the Amorphous Solid Dispersion of Curcumin: A Rational Selec-

tion of Polymers for Enhanced Solubility and Dissolution. Crystals 12: 1606. https://doi.org/10.3390/cryst12111606

Ismael QA, Hameed GS, Aziz FM (2020) Effect of introduction of polymers on the antibacterial activity of crystalline antibiotics. International Journal of Pharmaceutical Research 12: 3411–3430. https://doi.org/10.31838/ijpr/2020.12.03.483

Iyer R, Petrovska Jovanovska V, Berginc K, Jaklič M, Fabiani F, Harlacher C, Huzjak T, Sanchez-Felix MV (2021) Amorphous solid dispersions (asds): the influence of material properties, manufacturing processes and analytical technologies in drug product development. Pharmaceutics 13(10): 1682. https://doi.org/10.3390/pharmaceutics13101682

Jaafar IS, Radhi AAJJoAPE, Research, Jul-Sep (2020) Preparation and physicochemical characterization of cocrystals for enhancing the dissolution rate of glimepiride. 10: 69. https://doi.org/10.51847/ug8tPWC

Jermain SV, Brough C, Williams RO (2018) Amorphous solid dispersions and nanocrystal technologies for poorly water-soluble drug delivery – An update. International Journal of Pharmaceutics 535: 379–392. https://doi.org/10.1016/j.ijpharm.2017.10.051

Jia S, Ning S, Leng Y, Jing Q, Xu Z, Ren F (2022) Stabilizing effect of soluplus on erlotinib metastable crystal form in microparticles and amorphous solid dispersions. Polymers (Basel) 14(6): 1241. https://doi.org/10.3390/polym14061241

Kadhim ZJ, Rajab NA (2022) Formulation and characterization of glibenclamide nanoparticles as an oral film. International Journal of Drug Delivery Technology 12: 387–394.

Kaoud RM, Alwan MH, Amran M, Fawzi HA (2024) Design and optimization of pantoprazole sodium mucoadhesive hydrogel microcapsules for the healing of peptic ulcers. Pharmacia 71: 1–14. https://doi.org/10.3897/pharmacia.71.e118323

Kayaert P, Van den Mooter G (2012) An investigation of the adsorption of hydroxypropylmethyl cellulose 2910 5 mPa s and polyvinylpyrrolidone K90 around Naproxen nanocrystals. J Pharm Sci 101: 3916–3923. https://doi.org/10.1002/jps.23267

Khalil MR, Hameed GS, Hanna DB (2023) Preparation and evaluation of azithromycin as rectal suppository to treat bacterial infection of COVID-19. Iraqi Journal of Pharmaceutical Sciences 32: 60–70. https://doi.org/10.31351/vol32iss3pp60-70

Kim D, Kim Y, Tin Y-Y, Soe M-T-P, Ko B, Park S, Lee J (2021) Recent technologies for amorphization of poorly water-soluble drugs. Pharmaceutics 13: 1318. https://doi.org/10.3390/pharmaceutics13081318

Kim K-T, Lee J-Y, Lee M-Y, Song C-K, Choi J-H, Kim D-D (2011) Solid dispersions as a drug delivery system. Journal of pharmaceutical Investigation 41: 125–142. https://doi.org/10.4333/KPS.2011.41.3.125

Király M, Sántha K, Kállai-Szabó B, Pencz KM, Ludányi K, Kállai-Szabó N, Antal I (2022) Development and dissolution study of a β-galactosidase containing drinking straw. Pharmaceutics 14(4): 769. https://doi.org/10.3390/pharmaceutics14040769

Koh SK, Jeong JW, Choi SI, Kim RM, Koo TS, Cho KH, Seo KW (2021) Pharmacokinetics and diuretic effect of furosemide after single intravenous, oral tablet, and newly developed oral disintegrating film administration in healthy beagle dogs. BMC Vet Res 17: 295. https://doi.org/10.1186/s12917-021-02998-4

Ku MS (2008) Use of the biopharmaceutical classification system in early drug development. AAPS Journal 10: 208–212. https://doi.org/10.1208/s12248-008-9020-0

La Rocca M, Rinaldi A, Bruni G, Friuli V, Maggi L, Bini M (2022) New emerging inorganic–organic systems for drug-delivery: Hydroxyapatite@furosemide hybrids. Journal of Inorganic and Organometallic Polymers and Materials 32: 2249–2259. https://doi.org/10.1007/s10904-022-02302-3

Lateef S, Basim M, Mohammed A (2024) Effect of different variables on the formulation of sodium alginate beads. Al Mustansiriyah Journal of Pharmaceutical Sciences 24: 117–126. https://doi.org/10.32947/ajps.v24i2.1007

Lava SAG, Zollinger C, Chehade H, Schaffner D, Sekarski N, Di Bernardo S (2023) Diuretics in pediatrics. Eur J Pediatr 182: 2077–2088. https://doi.org/10.1007/s00431-022-04768-2

Lee J, Lee JJ, Lee S, Dinh L, Oh H, Abuzar SM, Ahn JH, Hwang SJ (2023) Preparation of apixaban solid dispersion for the enhancement of apixaban solubility and permeability. Pharmaceutics 15(3): 907. https://doi.org/10.3390/pharmaceutics15030907

Li M, Wang M, Liu Y, Ouyang R, Liu M, Han D, Gong J (2021) Co-amorphization story of furosemide-amino acid systems: Protonation and aromatic stacking insights for promoting compatibility and stability. Crystal Growth & Design 21: 3280–3289. https://doi.org/10.1021/acs.cgd.1c00015

Lomba L, Polo A, Alejandre J, Martínez N, Giner B (2023) Solubility enhancement of caffeine and furosemide using deep eutectic solvents formed by choline chloride and xylitol, citric acid, sorbitol or glucose. Journal of Drug Delivery Science and Technology 79: 104010. https://doi.org/10.1016/j.jddst.2022.104010

Maded ZK, Lassoued MA, Taqa GAA, Fawzi HA, Abdulqader AA, Jabir MS, Mahal RK, Sfar S (2024a) Topical Application of Dipyridamole and Roflumilast Combination Nanoparticles Loaded Nanoemulgel for the Treatment of Psoriasis in Rats. International Journal of Nanomedicine 19: 13113–13134. https://doi.org/10.2147/IJN.S492180

Maded ZK, Sfar S, Taqa GAA, Lassoued MA, Ben Hadj Ayed O, Fawzi HA (2024b) Development and optimization of dipyridamole- and roflumilast-loaded nanoemulsion and nanoemulgel for enhanced skin permeation: Formulation, characterization, and in vitro assessment. Pharmaceuticals 17(6): 803. https://doi.org/10.3390/ph17060803

Mahmood SZ, Yousif NZ, Salman ZD (2022) Types of attractive dosage forms for primary school students and associated factors in Baghdad/ Iraq. Al Mustansiriyah Journal of Pharmaceutical Sciences 20: 13–22. https://doi.org/10.32947/ajps.v20i4.770

Mahmoud ZH, Mahdi AB, Alnassar YS, Al-Salman H (2023) Formulation and sustained-release of verapamil hydrochloride tablets. The Chemist 76: 337–346.

Malkawi R, Malkawi WI, Al-Mahmoud Y, Tawalbeh J (2022) Current trends on solid dispersions: past, present, and future. Advances in Pharmacological and Pharmaceutical Sciences 2022: 5916013. https://doi.org/10.1155/2022/5916013

Martir J, Flanagan T, Mann J, Fotaki N (2020) In vivo predictive dissolution testing of montelukast sodium formulations administered with drinks and soft foods to infants. AAPS PharmSciTech 21: 282. https://doi.org/10.1208/s12249-020-01825-7

Masarone D, Valente F, Rubino M, Vastarella R, Gravino R, Rea A, Russo MG, Pacileo G, Limongelli G (2017) Pediatric heart failure: a practical guide to diagnosis and management. Pediatrics & Neonatology 58: 303–312. https://doi.org/10.1016/j.pedneo.2017.01.001

McMahon BA, Chawla LS (2021) The furosemide stress test: current use and future potential. Ren Fail 43: 830–839. https://doi.org/10.1080/0886022x.2021.1906701

Miller JM, Beig A, Carr RA, Spence JK, Dahan A (2012) A win-win solution in oral delivery of lipophilic drugs: Supersaturation via amorphous solid dispersions increases apparent solubility without sacrifice of intestinal membrane permeability. Molecular Pharmaceutics 9: 2009–2016. https://doi.org/10.1021/mp300104s

Monschke M, Wagner KG (2020) Impact of HPMCAS on the dissolution performance of polyvinyl alcohol celecoxib amorphous solid dispersions. Pharmaceutics 12(6): 541. https://doi.org/10.3390/pharmaceutics12060541

Mudrić J, Arsenijević J, Maksimović Z, Ibrić S, Gopčević K, Đuriš J (2021) Tablet and capsule formulations incorporating high doses of a dry optimized herbal extract: The case of Satureja kitaibelii. Journal of Drug Delivery Science and Technology 66: 102776. https://doi.org/10.1016/j.jddst.2021.102776

Müller D, Fimbinger E, Brand C (2021) Algorithm for the determination of the angle of repose in bulk material analysis. Powder Technology 383: 598–605. https://doi.org/10.1016/j.powtec.2021.01.010

Mustafa WW, Fletcher J, Khoder M, Alany RG (2022) Solid dispersions of gefitinib prepared by spray drying with improved mucoadhesive and drug dissolution properties. AAPS PharmSciTech 23: 48. https://doi.org/10.1208/s12249-021-02187-4

Muter SS, Habeeb ADJP (2025) Preparation and evaluation of gastroretentive floating unfolding film of baclofen. Pharmacia 72: 1–12. https://doi.org/10.3897/pharmacia.72.e147835

Naama NA, Hameed GS, Hanna DB, Mahdi ZH (2025) Formulation of cefdinir ternary solid dispersion and stability study under harsh conditions. Al Mustansiriyah Journal of Pharmaceutical Sciences 25: 27–48. https://doi.org/10.32947/ajps.v25i1.1106

Nandi U, Ajiboye AL, Patel P, Douroumis D, Trivedi V (2021) Preparation of solid dispersions of simvastatin and soluplus using a single-step organic solvent-free supercritical fluid process for the drug solubility and dissolution rate enhancement. Pharmaceuticals 14: 846. https://doi.org/10.3390/ph14090846

Newman A, Hastedt JE, Yazdanian M (2017) New directions in pharmaceutical amorphous materials and amorphous solid dispersions, a tribute to Professor George Zografi – Proceedings of the June 2016 Land O'Lakes Conference. AAPS Open 3: 7. https://doi.org/10.1186/s41120-017-0017-6

Newman A, Knipp G, Zografi G (2012) Assessing the performance of amorphous solid dispersions. Journal of Pharmaceutical Sciences 101: 1355–1377. https://doi.org/10.1002/jps.23031

Nser SM, Al-Shohani ADH, Abuawad A (2023) Effect of using high molecular weight crosslinker on the physical properties of super porous hydrogel composite. Al Mustansiriyah Journal of Pharmaceutical Sciences 23: 355–366. https://doi.org/10.32947/ajps.v23i4.1091

Nunn T, Williams J (2005) Formulation of medicines for children. Br J Clin Pharmacol 59: 674–676. https://doi.org/10.1111/j.1365-2125.2005.02410.x

Nupur MA, Rahman MM, Akter K, Hanif KB, Sharna JF, Sarker MS, Ibne Wahed MI (2023) Preparation and characterization of naproxen solid dispersion using different hydrophilic carriers and in-vivo evaluation of its analgesic activity in mice. Heliyon 9: e15432. https://doi.org/10.1016/j.heliyon.2023.e15432

Pandey M, Singh A, Namrata, Agnihotri N, Kumar R, Saha P, Pandey RP, Kumar A, Shiwangi (2022) Clinical pharmacology & therapeutic uses of diuretic agents: A review. Journal for Research in Applied Sciences and Biotechnology 1: 11–20. https://doi.org/10.55544/jrasb.1.3.3

Pantwalawalkar J, More H, Bhange D, Patil U, Jadhav N (2021) Novel curcumin ascorbic acid cocrystal for improved solubility. Journal of Drug Delivery Science and Technology 61: 102233. https://doi.org/10.1016/j.jddst.2020.102233

Pharmacopeia U (2018) The United States Pharmacopeia, USP 41/The National Formulary. In: Rockville, MD: US Pharmacopeial Convention.

Purandare S, Khot S, Avachat A (2024) Fabrication of pellets via extrusion-spheronization for engineered delivery of Famotidine through specialized straws for Paediatrics. Annales Pharmaceutiques Françaises. Elsevier, 271–284. https://doi.org/10.1016/j.pharma.2023.12.008

Ravikumar AA, Kulkarni PK, Osmani RAM, Hani U, Ghazwani M, Fatease AA, Alamri AH, Gowda DV (2022) Carvedilol precipitation inhibition by the incorporation of polymeric precipitation inhibitors using a stable amorphous solid dispersion approach: formulation, characterization, and in vitro in vivo evaluation. Polymers 14: 4977. https://doi.org/10.3390/polym14224977

Ruponen M, Kettunen K, Santiago Pires M, Laitinen R (2021) Co-amorphous formulations of furosemide with arginine and p-glycoprotein inhibitor drugs. Pharmaceutics 13: 171. https://doi.org/10.3390/pharmaceutics13020171.

S'Ari M, Blade H, Cosgrove S, Drummond-Brydson R, Hondow N, Hughes LP, Brown A (2021) Characterization of amorphous solid dispersions and identification of low levels of crystallinity by transmission electron microscopy. Mol Pharm 18: 1905–1919. https://doi.org/10.1021/acs.molpharmaceut.0c00918

Saboo S, Bapat P, Moseson DE, Kestur US, Taylor LS (2021) Exploring the role of surfactants in enhancing drug release from amorphous solid dispersions at higher drug loadings. Pharmaceutics 13(5): 735. https://doi.org/10.3390/pharmaceutics13050735

Sabry S, El hakim Ramadan A, Abd elghany M, Okda T, Hasan A (2021) Formulation, characterization, and evaluation of the anti-tumor activity of nanosized galangin loaded niosomes on chemically induced hepatocellular carcinoma in rats. Journal of Drug Delivery Science and Technology 61: 102163. https://doi.org/10.1016/j.jddst.2020.102163

Salunke S, Brandys B, Giacoia G, Tuleu C (2013) The STEP (Safety and Toxicity of Excipients for Paediatrics) database: part 2 - the pilot version. Int J Pharm 457: 310–322. https://doi.org/10.1016/j.ijpharm.2013.09.013

Salunke S, Giacoia G, Tuleu C (2012) The STEP (safety and toxicity of excipients for paediatrics) database. Part 1-A need assessment study. Int J Pharm 435: 101–111. https://doi.org/10.1016/j.ijpharm.2012.05.004

Saraf I, Roskar R, Modhave D, Brunsteiner M, Karn A, Neshchadin D, Gescheidt G, Paudel A (2022) Forced Solid-State Oxidation Studies of Nifedipine-PVP Amorphous Solid Dispersion. Mol Pharm 19: 568–583. https://doi.org/10.1021/acs.molpharmaceut.1c00678

Shah A, Atneriya UK, Joshi U, Solanki D (2024) Development and evaluation of pullulan based mouth dissolving film of furosemide. Fabad Journal of Pharmaceutical Sciences 49: 65–80. https://doi.org/10.55262/fabadeczacilik.1327446

Shariare MH, Altamimi MA, Marzan AL, Tabassum R, Jahan B, Reza HM, Rahman M, Ahsan GU, Kazi M (2019) In vitro dissolution and bioavailability study of furosemide nanosuspension prepared using design of experiment (DoE). Saudi Pharm J 27: 96–105. https://doi.org/10.1016/j.jsps.2018.09.002

Sica DA (2003) Pharmacotherapy in congestive heart failure: drug absorption in the management of congestive heart failure: loop diuret-

ics. Congest Heart Fail 9: 287–292. https://doi.org/10.1111/j.1527-5299.2003.02399.x

Simšič T, Nolimal B, Minova J, Baumgartner A, Planinšek O (2021) A straw for paediatrics: How to administer highly dosed, bitter tasting paracetamol granules. Int J Pharm 602: 120615. https://doi.org/10.1016/j.ijpharm.2021.120615

Sulaiman Hameed G, Basim Mohsin Mohamed M, Naji Sahib M (2022) Binary or ternary mixture of solid dispersion: Meloxicam case. Pharmacia 69: 801–808. https://doi.org/10.3897/pharmacia.69.e86744

Sutthapitaksakul L, Thanawuth K, Huanbutta K, Sriamornsak P (2022) Effect of a superdisintegrant on disintegration of orally disintegrating tablets determined by simulated wetting test and in vitrodisintegration test. Die Pharmazie-An International Journal of Pharmaceutical Sciences 77: 287–290.

Sweetman SC, Martindale C (2009) The complete drug reference. Vol. 1, Pharmaceutical press London.

Tadauchi T, Yamada D, Koide Y, Yamada M, Shimada Y, Yamazoe E, Ito T, Tahara K (2022) Improving the powder properties of an active pharmaceutical ingredient (Ethenzamide) with a silica nanoparticle coating for direct compaction into tablets. Powders 1: 231–242. https://doi.org/10.3390/powders1040016

Tekade AR, Yadav JN (2020) A review on solid dispersion and carriers used therein for solubility enhancement of poorly water soluble drugs. Advanced Pharmaceutical Bulletin 10: 359–369. https://doi.org/10.34172/apb.2020.044

Todaro V, Healy AM (2021) Development and characterization of ibuprofen co-crystals granules prepared via fluidized bed granulation in a one-step process – a design of experiment approach. Drug Development and Industrial Pharmacy 47: 292–301. https://doi.org/10.1080/03639045.2021.1879836

Tong M, Wu X, Zhang S, Hua D, Li S, Yu X, Wang J, Zhang Z (2022) Application of TPGS as an efflux inhibitor and a plasticizer in baicalein solid dispersion. European Journal of Pharmaceutical Sciences 168: 106071. https://doi.org/10.1016/j.ejps.2021.106071

Tung N-T, Tran C-S, Nguyen T-L, Pham T-M-H, Chi S-C, Nguyen H-A, Bui Q-D, Bui D-N, Tran T-Q (2021) Effect of surfactant on the in vitro dissolution and the oral bioavailability of a weakly basic drug from an amorphous solid dispersion. European Journal of Pharmaceutical Sciences 162: 105836. https://doi.org/10.1016/j.ejps.2021.105836

Vaid V, Jindal R (2022) RSM-CCD optimized in air synthesis of novel kappa-carrageenan/tamarind kernel powder hybrid polymer network incorporated with inclusion complex of (2-hydroxypropyl)-β-cyclodextrin and adenosine for controlled drug delivery. Journal of Drug Delivery Science and Technology 67: 102976. https://doi.org/10.1016/j.jddst.2021.102976

Vaka SRK, Bommana MM, Desai D, Djordjevic J, Phuapradit W, Shah N (2014) Excipients for Amorphous Solid Dispersions. In: Shah N, Sandhu H, Choi DS, Chokshi H, Malick AW (Eds) Amorphous Solid Dispersions: Theory and Practice. Springer New York, New York, NY, 123–161. https://doi.org/10.1007/978-1-4939-1598-9_4

Van Den Mooter G (2012) The use of amorphous solid dispersions: A formulation strategy to overcome poor solubility and dissolution rate. Drug Discovery Today: Technologies 9: e79–e85. https://doi.org/10.1016/j.ddtec.2011.10.002

Van der Merwe C (2021) Improvement of the pharmaceutical availability and membrane permeability of furosemide by formulation design. North-West University (South-Africa).

Vasconcelos T, Marques S, das Neves J, Sarmento B (2016) Amorphous solid dispersions: Rational selection of a manufacturing process. Advanced Drug Delivery Reviews 100: 85–101. https://doi.org/10.1016/j.addr.2016.01.012

Vasconcelos T, Prezotti F, Araújo F, Lopes C, Loureiro A, Marques S, Sarmento B (2021) Third-generation solid dispersion combining Soluplus and poloxamer 407 enhances the oral bioavailability of resveratrol. International Journal of Pharmaceutics 595: 120245. https://doi.org/10.1016/j.ijpharm.2021.120245

Vasconcelos T, Sarmento B, Costa P (2007) Solid dispersions as strategy to improve oral bioavailability of poor water soluble drugs. Drug Discovery Today 12: 1068–1075. https://doi.org/10.1016/j.drudis.2007.09.005

Vo CLN, Park C, Lee BJ (2013) Current trends and future perspectives of solid dispersions containing poorly water-soluble drugs. European Journal of Pharmaceutics and Biopharmaceutics 85: 799–813. https://doi.org/10.1016/j.ejpb.2013.09.007

Walden DM, Bundey Y, Jagarapu A, Antontsev V, Chakravarty K, Varshney J (2021) Molecular Simulation and Statistical Learning Methods toward Predicting Drug-Polymer Amorphous Solid Dispersion Miscibility, Stability, and Formulation Design. Molecules 26: https://doi.org/10.3390/molecules26010182

Wlodarski K, Zhang F, Liu T, Sawicki W, Kipping T (2018) Synergistic effect of polyvinyl alcohol and copovidone in itraconazole amorphous solid dispersions. Pharm Res 35: 16. https://doi.org/10.1007/s11095-017-2313-1

Wu L, Rodriguez M, El Hachem K, Krittanawong C (2024) Diuretic treatment in heart failure: A practical guide for clinicians. Journal of Clinical Medicine 13: 4470. https://doi.org/10.3390/jcm13154470

Yu C, Zhang C, Guan X, Yuan D (2023) The solid dispersion of resveratrol with enhanced dissolution and good system physical stability. Journal of Drug Delivery Science and Technology 84: 104507. https://doi.org/10.1016/j.jddst.2023.104507

Yu DG, Li JJ, Williams GR, Zhao M (2018) Electrospun amorphous solid dispersions of poorly water-soluble drugs: A review. J Control Release 292: 91–110. https://doi.org/10.1016/j.jconrel.2018.08.016

Zahálka L, Klovrzová S, Matysová L, Šklubalová Z, Solich P (2018) Furosemide ethanol-free oral solutions for paediatric use: formulation, HPLC method and stability study. Eur J Hosp Pharm 25: 144–149. https://doi.org/10.1136/ejhpharm-2017-001264

Zhang F, Mao J, Tian G, Jiang H, Jin Q (2022) Preparation and characterization of furosemide solid dispersion with enhanced solubility and bioavailability. AAPS PharmSciTech 23: 65. https://doi.org/10.1208/s12249-022-02208-w

Zhang L, Yue L-N, Sui Y-L, Zhao Y, Ding X, Li Q, Zhang C, Wu C, Gao C, Qian J-Y (2021) Regulating the mechanical properties and microporous structures of hydroxypropyl methylcellulose based microporous photophobic films by adjusting the l-ethyl-3-methylimidazolium acetate content. Progress in Organic Coatings 155: 106226. https://doi.org/10.1016/j.porgcoat.2021.106226

Zhou Z, Chen J, Zhang Z-x, Wang F-b, Wang L, Lin Y, Zhang X, Liu J (2022) Solubilization of luteolin in PVP40 solid dispersion improves inflammation-induced insulin resistance in mice. European Journal of Pharmaceutical Sciences 174: 106188. https://doi.org/10.1016/j.ejps.2022.106188